University of Venda

CLAY POLYMER NANOCOMPOSITES AS FLUORIDE ADSORBENT IN GROUNDWATER

Masters research, University of Venda, School of Environmental Sciences, Department of Ecology and Resource Management

By

Thendo Dennis Nengudza

11591576

Supervisor: Prof. Gitari W.M (University of Venda)

Co-supervisor: Dr. Kayembe J.D (University of the Witwatersrand)

DECLARATION

I, Nengudza Thendo Dennis hereby declare that **"Clay polymer nanocomposites as fluoride adsorbent in groundwater"** for the bachelor of environmental sciences master's degree submitted at the University of Venda is my own work. I clearly sate that this dissertation has not been submitted previously for a degree at this or any other institution, moreover, I swear that this is my own work in design and execution and as thus, all reference materials and resources has been duly acknowledged.

Signature..... Date.....

ACKNOWLEDGMENTS

I would like to acknowledge and thank the following for their generous contribution to the success of this research work:

My supervisor, **Professor Gitari. W.M.** for your endless patients and encouragement, to whom I am indebted to for the dedicated, detailed expert guidance and financial assistance he offered me during the preparation and compilation of the project.

My sincere gratitude to my co-supervisor **Dr. Kayembe J.D** for his conceptual contribution

My colleagues and fellow students in the Environmental Remediation and Pollution Chemistry Research Group members, especially Mr Mudzielwana R., Mr Pindihama G., and Obijole O., for their valuable assistance and motivation.

Mr Nengudza M.E. and **Mrs Nengudza T.J.** my parents for their support, love and care.

ABSTRACT

Fluoride is one of the anionic contaminants which is found in excess in groundwater because of geochemical reaction or anthropogenic activities such as the disposal of industrial wastewaters. Among various methods used for defluoridation of water such as precipitation, ion-exchange processes, membrane processes, the adsorptions process is widely used. It offers satisfactory results and seems to be a more attractive method for the removal of fluoride in terms of cost, simplicity of design and operation.

In this work, the preparation of clay polymer nanocomposites (CPNCs) used in defluoridation began by modifying the original natural Mukondeni clay to render the layered silicate miscible with the chosen polymer, microcrystalline cellulose. Clay polymer nanocomposites (CPNCs) were synthesized using the melt intercalation method. Mukondeni black clay with microcrystalline cellulose as polymers was melt mixed at 220 °C for 10 minutes in an extruder for exfoliation of the resulting composite. Physicochemical characteristics and mineralogical characteristics of the CPNC was determined using XRD, XRF, BET, FTIR and SEM. Batch adsorption experiments were conducted to determine the efficiency of CPNCs in defluoridation of groundwater. The pH, EC, TDS and fluoride concentration of field water was determined using the CRISON MM40 multimeter probe and the Orion versastar fluoride selective electrode for fluoride concentration.

Elemental analysis revealed that CPNC 1:1 is mainly characterized of cellulose, Quartz and Albatite as the major minerals with traces of Montmorillonite, Ednite and Magnesium as minor minerals constituting CPNC 1:1. The structure of 1:4 CPNC was partially crystalline and partially amorphous showing increased cellulose quantity (1:4 clay to cellulose) as compared 1:1 CPNC, 1:2 CPNC and 1:3 CPNC.

Maximum adsorption of fluoride was attained in 10 minutes using 0.5g of 1:4 CPNC removed 22.3% of fluoride. The initial fluoride concentration for the collected field groundwater was 5.4 mg/L, EC 436 µS/cm, and TDS 282 mg/L. The regeneration potential of CPNCs was evaluated through 3 successive adsorption desorption cycles. Fluoride removal decreased after the first cycle for all ratios of CPNCs, a continued decreased can be observed following the second cycle. CPNC 1:2 decreased from 9.32 % at the 1st cycle to 2.84 % and 0.56 % on the 2nd and 3rd cycle respectively. CPNC 1:4 decreased from 8.22 % at the 1st cycle to 4.80 % and 0.72 % on the 2nd and 3rd cycle respectively. The fluoride-rich Siloam groundwater had a slightly alkaline pH of 9.6.

The low adsorptive characteristic displayed by all 4 CPNCs can be deduced from the BET analysis that revealed low surface area, pore volume, and pore size, it is evident from the BET analysis that less fluoride will be absorb as adsorption sites will be limited.

Based on the findings of this study, recommendations are designing of correct preparation techniques to obtain nanocomposites with desirable properties, polymer melting points and evaporation point of the binder should be taken into consideration.

Key words: groundwater, fluoride, adsorption, nanocomposites, cellulose, Mukondeni clay

ACRONYMS AND ABBREVIATIONS

BET: Brunauer-Emmett Teller

CEC: Cation exchange capacity

CPNC: Clay polymer nanocomposites

EC: Electrical Conductivity

EDS: Energy dispersive spectroscopy

FTIR: Fourier transform infrared spectroscopy

LOI: Loss on Ignition

pH: Potential Hydrogen

SEM: Scanning electron microscopy

TEM: Transmission electron microscopy

TDS: Total Dissolved Solids

TGA: Thermogravimetric analysis

WHO: World Health Organization

XRD: X-ray diffraction

XRF: X-ray fluorescence

NOTE: Please refer to the periodic table for the elements

Table of Contents

LIST OF FIGURES

LIST OF TABLES

LIST OF EQUATIONS

CHAPTER ONE

Introduction

1.1 Background

One of the biggest challenges of the 21st century is to ensure adequate safe drinking water supplies in rural communities around South Africa and worldwide. Clean drinking water is one of the implicit requisites for a healthy human population. However, the growing industrialisation, and extensive use of chemicals for various concerns, has increased the burden of unwanted pollutants of drinking water in developed and developing countries all over the world *(Srinivasan, et al., 2011).* Among the various undesirable and naturally occurring pollutants in water, coliform bacteria, heavy metals (arsenic, cadmium, chromium, lead and selenium), nitrates and nitrites, and fluoride are very important as they cause serious health problems *(Mroczek, et al., 2005)*. Fluoride contamination in groundwater due to natural and anthropogenic activities has been recognized as one of the major problems worldwide posing a serious threat to human health *(Bhatnagar, et al., 2011).*

Fluoride concentrations in groundwater of some places in the world exceed the acceptable value. In South Africa, areas of Northern Cape, North West, KwaZulu-Natal and Limpopo are mainly characterized by sedimentary, granite, metamorphic and volcanic rocks which contain fluoride hence contamination of groundwater is possible (Ncube, 2002). The optimum fluoride level in drinking water for general good health set by World Health Organisation (WHO) is considered to be between 0.5 and 1.0 mg/l *(Srimurali, et al., 1998).*

The conventional approaches for fluoride removal from water include chemical precipitation, ion exchange, adsorption, electro-dialysis, Donnan dialysis and reverse osmosis *(Hichour, et al., 2000; Lou and Inoue, 2004; Ndiaye, et al., 2005; Biswas, et al., 2007; Sujana, et al., 2009)*. Among all these methods, adsorption technique is economically favourable and technically feasible to separate fluoride from aqueous solutions as the requirement of operative controls are minimal (Raichur and Basu, 2001).

Smectites are a valuable mineral for industrial and academic applications because of their high cation exchange capacities, surface area, surface reactivity and their adsorptive properties *(Suprakas, et al., 2003)*. A study done by Gitari et al, 2013, used bentonite clay (smectite type clay) in the removal of excess fluoride from groundwater, the adsorption capacity of fluoride by 1 g of modified bentonite clay was observed to be 5.7 mg g^{-1} at room temperature. Studies on conventional clay composite have been done by different researchers in efforts of removing

fluoride from water. Most of these studies do remove fluoride to an acceptable level i.e. <1.5 mg/L. Mandal, et al., 2008, used cellulose supported layered hydroxide for the adsorption of fluoride revealing that cellulose supported layered hydroxide is an excellent material for adsorption of fluoride from aqueous solution.

Since the 18th century, CPNCs (clay polymer nanocomposites) have been intensely researched due to the performance improvement achieved when small amount of silicate particles are added to a polymer matrix. The remarkable change on physical and mechanical properties of polymers due to the addition of inorganic solids is explained by the huge surface area *(Oliveira, et al., 2013).* CPNCs are a typical example of nanomaterial that can be used in fluoride removal from groundwater intended for domestic use. This class of material uses smectite-type clays, such as hectorite, montmorillonite, and mica, as fillers to enhance the properties of polymers. Smectite type clays have a layered structure *(Masami, et al., 2003).* Each layer is constructed from tetrahedrally coordinated Si atoms fused into an edge shared octahedral plane of either Al(OH)3 or Mg(OH)2. CPNCs often have properties that are superior to conventional micro-scale composites because of the strong interaction between components and can be synthesized using simple and inexpensive techniques *(Mangala, et al,. 2006).*

Clay polymer layered silicate nanocomposites show superior physical, mechanical and chemical properties (e.g. 40% increased tensile strength at room temperature), improved resistance, chemical resistance, and gas barrier (100-fold decrease in O_2 and H_2O permeability) compared to conventional composites. The layered silicates (alternatively referred to as 2:1 layered aluminosilicates, phyllosilicates, clay minerals and smectites) are the most commonly used inorganic nano elements in polymer nanocomposites research to date *(Vaia, et al., 2002).* This makes layered silicate in clay polymer composites suitable candidates in fluoride removal from groundwater as fluoride is adsorbed onto clays (smectite, palygorskite, illite, and kaolinite) in ion-exchange reaction where the fluoride ion (F^-) competes with hydroxyl ions (OH^-), but the primary reaction appears to be highly supplemented by the high surface area of the polymer clay nanocomposite *(Fluhler, et al., 1982).*

The preparation of polymer/clay nanocomposites with good dispersion of clay layers within the polymer matrix is not possible by physical mixing of polymer and clay particles (Pavildou and Papasspyrides, 2008).

The intrinsic incompatibility of hydrophilic clay layers with hydrophobic polymer chains prevents the dispersion of clay nanolayers within polymer matrix and causes weak interfacial

interactions. Incompatibility and weak interfacial interactions hinders the exfoliation and preparation of dispersed stable nanocomposite with improved properties. Modification of clay layers with hydrophobic agents is necessary in order to render the clay layers more compatible with polymer chains. This is surface modifications which causes the reduction of surface energy of clay layers and match their surface polarity with polymer polarity. The organoclays with lowered surface energy are more compatible with polymers and polymer molecules are able to intercalate within their interlayer space or galleries under well-defined experimental conditions *(Ali, et al., 2011).*

The surface modification of clay layers can be achieved through a cation exchange process by the replacement of sodium and calcium cations present in the inter layer space or clay galleries by alkylammonium or alkylphosphonium (onium) cations *(Ahmad et al., 2009).* In addition to the surface modification and increasing the hydrophobicity of clay layers, the insertion of alkylammonium or alkylphosphonium cations into the galleries causes to some degree increase in the interlayer spacing which promotes intercalation of the polymer chains into the galleries during nanocomposite preparation *(Chigwada et al., 2006).* Also the alkylammonium or alkylphosphonium cations can provide functional groups which interact with polymer chains or initiate the polymerization and therefore increase the interfacial interactions.

1.2 Problem statement

The presence of naturally occurring fluorides or added fluoridated salts in drinking water allows its easy entrance in the body via the gastrointestinal tract *(Viswanathan, et al., 2010).* Epidemiological studies reveal that drinking water is the major source of fluoride daily intake, and continuous consumption of drinking water with heightened fluoride concentrations (>1.5 mg/L) can induces birth, reproduction and immunological defects *(Valdez-Jimenez, et al., 2011),* dental and skeletal fluorosis *(Mandinic, et al., 2010).* Though small concentration of fluoride is essential for normal mineralization of bones and the formation of dental enamel *(Fung, et al., 1999),* excessive intake of fluoride causes dental enamel to lose its lustre into either mild form of the more common effect, dental fluorosis, which is characterized by white, opaque areas on tooth surface, and yellow brown to black stains on the teeth (Choubasia and Sompura, 1996).

Excessive intake may also result in slow, progressive crippling scourge known as skeletal fluorosis. The degree of fluorosis depends on the amount and concentration of fluoride intake; children under the age of 10 are more vulnerable to both dental and skeletal fluorosis when

exposed to high levels of fluoride intake. Fluoride mainly gets deposited in joints of the neck, knee, pelvis and shoulder and makes it difficult to move or walk. An advanced stage of osteoporosis in long bones and bony outgrowth may occur, vertebrae may fuse together and a victim may be crippled (Meenakshi and Maheshwari, 2006). These negative health effects of fluoride are permanent and irreversible (Rajgopal and Tobin, 1991).

1.3 Objectives

1.3.1 General objectives

The main objective of this study was to synthesize a clay polymer nanocomposites (CPNC) using Mukondeni black clay and cellulose and assess its capacity to remove fluoride from groundwater.

1.3.2 Specific objectives

- To optimize the modification of clay layers.
- To determine the chemical and mineralogical properties of free Mukondeni black clay, cellulose and the synthesized clay polymer nanocomposite i.e. chemical composition and mineralogy, cation exchange capacity, point of zero charge and surface area.
- To evaluate the optimum conditions and adsorption capacity of fluoride onto the synthesized clay polymer nanocomposite i.e. contact time, pH, adsorbent dose and adsorbate dose.
- To evaluate the regeneration potential of the synthesized clay polymer nanocomposite.

1.4 Delimitations of the research and the study

Groundwater can become contaminated from natural sources. Some substances found naturally in rocks or soils such as iron, manganese, arsenic, chloride, sulfates or radionuclides, can become dissolved in groundwater and contamination can occur. This study will only investigate the efficiency of CPNCs in removing fluoride from groundwater

1.5 Significance and justification of the study

The significance and motive of this study is to make full use of and derive benefits from the tremendous improvements in a wide range of physical, mechanical and chemical properties offered by CPNCs as compared to those of conventional clay composites. Clay polymer composites and nanocomposites have gained increasing attention worldwide academically as well as industrially due to the superior properties they exhibit compared to either the clay or the polymer.

CHAPTER TWO

Literature Review

2.1 Fluoride

Fluorine (F_2) is a pale, yellow-green, corrosive gas which almost cannot be found in natural environment in elemental form due to its high electronegativity and reactivity. Fluorine readily forms compounds with other elements and commonly occurs as fluoride in aqueous solution. Regarding chemical aspects, fluorine is the 13th most abundant element. Fluoride (F^-) is a fluorine anion characterized by small radius, great tendency to behave as ligand and easiness to form a great number of different organic and inorganic compounds in soil, rocks, air, plants and animals. Some of those compounds are quite soluble in water, so fluoride is present in surface and groundwater as an almost completely dissociated fluoride ion (WHO, 2002).

Fluoride (F^-) is one of the most ubiquitous inorganic water contaminants in groundwater around the world, due to its easy dissolution from underground rocks that contain it (AWWA, 1999). In the solid state, fluoride is always associated with metals. At pH values lower than 5, fluoride associates with the hydrogen ion (H^+) to form the HF molecule and the complex HF_2 *(Boruff, et al., 1934)*. It can be released into the environment naturally in both water and air. In aqueous solution, fluoride can be found as either free ion or joined to metals/metalloids in complexes forms.

2.1.1 Origin and occurrence of fluoride in the environment

Fluorides are found in varying amounts in practically all the geological formations, especially in most igneous rocks (M'Caffrey, 1993; Fayazi, 1994). The presence of fluoride in groundwater is considered as an endemic problem in at least 25 countries worldwide including South Africa. The problem of high-fluoride ion concentrations in groundwater is one of the most important health-related issues worldwide *(Gupta, et al., 2007)*. It is there for important to manage fluoride at acceptable levels in our water resources. For this to happen, there must be proper understanding of the occurrence, factors that contribute to the release of fluoride into groundwater, influence of the fluoride ion concentration once it is in groundwater and hence the distribution of different levels of fluoride in groundwater (Saha, 1993). Fluorine occurs naturally in the earth's crust where it can be found in rocks, coal and clay. Known fluoride belts on land include: one that stretches from Syria through to Jordan, Egypt, Libya, Algeria, Sudan, Kenya and Tanzania, and other that stretch from Turkey through Iraq, Iran, Afghanistan, India,

Northern Thailand and China. There are similar belts in the Americas and Japan *(Menda, et al., 2004).*

Fluorides are released into the environment naturally through the weathering of minerals, in emissions from volcanoes and in marine aerosols *(Symonds, et al., 1988).* The main natural source of inorganic fluorides in soil is the parent rock (WHO, 1984). During weathering, some fluoride minerals (e.g. cryolite, or Na^3AlF_6) are rapidly broken down, especially under acidic conditions (Fuge and Andrews, 1988). Other minerals, such as fluorapatite ($Ca_5(PO_4)3F$) and calcium fluoride, are dissolved more slowly (Kabata-Pendias & Pendias, 1984). The mineral fluorophlogopite (mica; $KMg^3(AlSi_3O_{10})F_2$) is stable in alkaline and calcareous soils (Elrashidi and Lindsay, 1986). However, its solubility is affected by pH and the activities of silicic acid (H_4SiO_4), aluminium (Al^{3+}), potassium (K^+) and magnesium (Mg^{2+}) ions.

Ionic compounds of fluoride dissolvein water and these are believed to be the cause of fluoride release into groundwater. The dissolution of other F^- bearing alumina silicate minerals has also been reported (WRC, 2001). During the mineralization of various fluoride rich minerals, solubility plays an important role. Table 1 below shows the solubility products (Ksp) values of some minerals relevant to the chemistry of groundwater (Gaciriand Davies, 1993).

Table 1: Solubility products for some minerals

Mineral	**Ksp**	**Temp. °C**
Fluorite (CaF_2)	3.4×10^{-11}	18 °C
Calcite ($CaCO_3$)	1×10^{-8}	25°C
Aragonite ($CaCO_3$)	1×10^{-8}	25 °C
OH^- apatite	2.6×10^{-45}	18 °C
OH^- apatite	2.3×10^{41}	40 °C
Selaite (MgF_2)	6.4×10^{-9}	27 °C
Halite (NaCl)	38 OR $1 \times 10^{1.58}$	25 °C
Siderite ($FeCO_3$)	$1 \times 10^{-10.5}$	25 °C
Magnesite ($MgCO_3$)	1×10^{-5}	25 °C

Dolomite	1 X $10^{-16.7}$	25 °C

According to Smedley, (1996), the concentrations of fluoride in groundwater have been shown to be limited by the mineral's solubility especially fluorite, such that in the presence of 10^{-3} M of calcium, the fluoride ion concentration is limited to 3.1 mg/L of fluoride. It is therefore the absence of calcium in solution which allows higher concentrations to be stable. High fluoride ion concentrations may therefore be expected in groundwater in calcium-poor aquifers and in areas where fluoride-bearing minerals are common.

2.1.2 Fluoride and human health

Many water quality assessment and epidemiological studies of possible adverse effects of long-term ingestion of fluoride via drinking water have been carried out (Chen, 1993; M'Caffrey, 1993, 1993; DWAF, 1996; Ogera, 1997; Guo and Wang, 1998; Muller, et al., 1998). Depending on its concentration, fluoride in drinking water is known for both beneficial and detrimental effects on human health, particularly to infants and young children. Fluoride ingestion in low concentration (between 0.5 and 1.5 mg/L) is recommended as prevention of dental caries. However, when fluoride is ingested in quantities that exceeds WHO guidelines (i.e. >1.5 mg/L), it permanently deposits on teeth and bones, which causes calcium deficiency and abnormal growth of bones. The most frequent diseases due to the excessive ingestion of fluoride are dental fluorosis (ingestion of water containing 1.5 to 4 mg L-1) and skeletal fluorosis (ingestion of water containing > 4 mg L-1) (BGS, 2000).

Approximately 75-90% of ingested fluoride is absorbed within the body (DWAF, 1996). In an acidic stomach, fluoride is converted into hydrogen fluoride (HF) and up to about 40% of the ingested fluoride is absorbed from the stomach as HF (Clair, et al., 1994). High stomach pH decreases gastric absorption by decreasing the concentration of HF. Fluoride not absorbed in the stomach is absorbed in the intestine and is unaffected by pH at this site (Whitford, 1997). Relative to the amount of fluoride ingested, high concentrations of cations that form insoluble complexes with fluoride (e.g. calcium, magnesium and aluminium) can markedly decrease gastrointestinal fluoride absorption (Whitford, 1997). When water-containing fluoride is consumed, some fluoride is retained by fluids in the mouth and is incorporated onto the teeth by surface uptake (topical effect). The rest enters the stomach where it is rapidly adsorbed by diffusion through the stomach walls and intestines. Fluoride enters the blood plasma and is

rapidly distributed throughout the body, including the teeth (systemic effect) (Clair, et al., 1994).

While there are a variety of ways of describing dental fluorosis, Dean's 1942 description is still extremely useful and widely used in epidemiological studies (Brouwer, 1988;Du Plessis, 1995).

Table 2: Dental Fluorosis Categorisation (Dean, 1942a)

Normal	The enamel presents the usual translucent, semi-vitriform type of structure. The surface is smooth, glossy and usually of a pale creamy white colour
Questionable	The enamel discloses slight aberrations from the translucency of normal enamel, ranging from a few white flecks to occasional white spots. This classification is used in those instances where a definite diagnosis of the mildest form of fluorosis is not warranted and a classification of "normal" not justified.
Very mild	Small, opaque, paper-white areas scattered irregularly over the tooth, but involving less than approximately 25% of the tooth surface. Frequently included in this classification are teeth showing no more than 1-2mm of white opacity at the tip of the summit of the cusps of the bicuspids or second molars?
Mild	The white opaque areas in the enamel of the teeth are more extensive but do not involve as much as 50% of the tooth.
Moderate	All enamel surfaces of the teeth are affected, and surfaces subject to attrition show marked wear. Brown stain is frequently a disfiguring feature.
Severe	Includes teeth formerly classified as "moderately severe" and "severe". All enamel surfaces are affected and hypoplasia is so marked that the general form of the tooth may be altered. The major diagnostic sign of this classification is the discrete or confluent pitting.

	Brown stains are widespread and teeth often present a corroded-like appearance.

Fluoride effects on bone tissues have been found to be cumulative and manifests in several stages with the less serious occurring early in the natural course of the disease. Whatever may be the type of fluoride exposure, the clinical picture in chronic poisoning occurs in the following phased manner (Dean, 1942b).

Table 3: Phases of Skeletal fluorosis

Preclinical phase	Asymptomatic, slight radiographically detectable increases in bone mass.
Phase □ of Preclinical phase	Musculoskeletal: sporadic pain, stiffness of joints, osteosclerosis of pelvis and spine.
Phase □ of Preclinical phase	Degenerative and destructive: chronic joint, arthritic symptoms, slight calcification of ligaments, increased osteoclerosis.
Phase □ of Preclinical phase	Crippling fluorosis: limitation of joint movement, calcification of ligaments/neck, spinal column, crippling deformities/spine and major joints, muscle wasting, neurological defects/compression of the spinal cord.

WRC, (2001), amongst other effects reported chronic effects on the kidneys in persons with renal disorders including effects on the thyroid gland, which may occur with long term-exposure to high fluoride concentrations.

Due to the detrimental effect of fluoride to human health when ingested in excessive amounts, studies around the world have been conducted for defluoridation purposes in efforts to minimize the harmful and irreversible effects of fluoride on human health.

2.2 Defluoridation methods and techniques

Considering the fact that fluorosis is an irreversible condition and has no cure, prevention is the only solution for this common most evident disease of the effects of high fluoride content in drinking water. In efforts of providing water with optimal fluoride concentration,

defluoridation was the convention and widely tested method for removing access fluoride in water

Defluoridation techniques can be broadly classified into four categories; Adsorption technique, Precipitation technique, Ion-exchange technique, and other techniques, which include Membrane processes, electro chemical defluoridation and Reverse Osmosis *(Piddennavar, et al., 2013).*

2.2.1 Adsorption

In the adsorption method, raw fluoridated water is passed through a bed containing defluoridating material. The material retains fluoride either by physical, chemical or ion exchange mechanisms. The adsorbent gets saturated after a period of operation and requires regeneration *(Lyengar, et al., 1996).*

A wide range of materials has been tried for fluoride uptake. Bauxite, magnetite, kaolinite, serpentine, various types of clays and red mud are some of the naturally occurring materials studied. The general mechanism of fluoride uptake by these materials is the exchange of metal lattice hydroxyl or other anionic group with fluoride. Fluoride uptake capacity can be increased by certain pre-treatments like acid washing and calcinations *(Lyengar, et al., 1996).*

In a study done by Mariappan (2011), clay pots are subjected to heat treatment as in the case of brick production. Hence the clay pot also will act as an adsorbent media. As per treatability-study results a marginal reduction in water fluoride level from 1.8 mg/L to 1.5 and 1.4 mg/L at the end of 2 days and 4 days respectively, which is practically not significant. Fluoride removal capacity will vary with respect to the alumina content present in the clay used for pot production. In a practical sense the use of clay pots for defluoridation is not promising. However, people can be advised to use clay pots to store water that is treated by other techniques, which results in partial defluoridation. The major advantages of clay pots are they are economic and readily acceptable for the rural communities.

2.2.2 Precipitation co-precipitation

According to Langmuir (1997) adsorption and co-precipitation have been widely described as two active mechanisms to trap contaminants from natural and polluted waters where a solute that would normally remain dissolved in a solution precipitates out on a carrier that forces it to bind together, rather than remaining dispersed.

Precipitation methods involve the addition of chemicals and the formation of fluoride precipitates or co-precipitates. Of the available precipitation methods the Nalgonda technique

which involves a direct addition of alum and lime depending on the fluoride content of water is the commonly used technique *(Frankel, et al., 1980).*

Co-precipitation can also be used as a synthesis method for fluoride adsorbents, in the novel study done by Chen, et al., 2011, Fe—Ti oxide adsorbent was synthesized by co-precipitation. The synergistic interactions between Fe and Ti both during crystallization and fluoride adsorption were investigated. The synthesized adsorbent had a high adsorption capacity and was cost effective.

The precipitation method is also used in fluoride removal in the treatment of significant amounts of fluoride waste discharge streams from a number of industries (semiconductor, photovoltaic, glass manufacturers, electroplating, steel and aluminum, pesticides and fertilizer), the fluoride concentration in effluent can vary over a large range, and the allowable level for discharge depends on the place of disposal *(Oke, et al., 2011).* When there is any risk of fluoride seeping back to water supplies, a limitation of around one mg/L fluoride is typical. High levels of fluoride are generally reduced by adding calcium salts, causing precipitation of CaF2. However these saturated CaF2 solutions must undergo further treatment. There are two known treatment processes: 1) Adsorption on activated alumina 2) Removal by selective ion exchange resin

2.2.3 Ion-exchange

Fluoride can be removed from water supplies with a strong basic anion-exchange resin containing quarternary ammonium functional groups. The removal takes place according to the following reaction *(Amor, et al., 2001)*:

Matrix- NR3+Cl- + F- → Matrix- NR3+F- + Cl-

Where in: R, and R3 are independently: methyl; a linear, branched, or cyclic, saturated, or unsaturated alkyl group containing one to ten carbon that may be substituted with one or more –OH, R3 is an acyl or thioacyl residue forming an amide with N.

The fluoride ions replace the chloride ions of the resin. This process continues until all the sites on the resin are occupied. The resin is then backwashed with water that is supersaturated with dissolved sodium chloride salt. New chloride ions then replace the fluoride ions leading to recharge of the resin and starting the process again. The driving force for the replacement of

chloride ions from the resin is the strong electronegativity of the fluoride ions *(Ogumi, et al., 1984)*.

A study done by Oke, 2011, et al., used a chelating resin loaded with aluminium ions for the fluoride exchange resin. The functional group of the resin is an amino-methyl-phosphonic-acid-group. It is significant that the aluminum ion is connected with the amino-methyl-phosphonic-acid -group, while the aluminum core is attached to one chloride ion. In contact with fluoride containing solutions the chloride is exchanged by fluoride. Other ions such as sulfate or nitrate do not interact with the aluminum ion since their affinity to aluminum is very low. However, this fluoride removal method cannot be used for portable drinking water but rather is an industrial method used to remove access fluoride in effluents from industries.

2.2.4 Membrane process

Membrane processes studied in the context of fluoride removal include reverse osmosis (Sehn, 2007), nanofiltration *(Elazhar et al., 2009)*, electrodialysis *(Amor et al., 2000)*, and Donnan dialysis *(Hichour et al., 2000)*. Membrane processes remove more fluoride than other technologies *(Ayoob et al., 2008).*

Reverse Osmosis (RO) is a technique that forces a solvent through a semipermeable membrane by applying pressure greater than the osmotic pressure of the solution. Membrane filtration processes remove particulate constituents based on size exclusion, but reverse osmosis does not. Reverse osmosis is able to reject constituents due to electrostatic repulsion at the membrane surface, chemical solubility, diffusivity and straining of solutes (Boysen, 2008).

Nano-filtration is a relatively low pressure process that removes primarily the larger dissolved solids as compared to reverse osmosis (Boysen, 2008).

Electrodialysis (ED) is a membrane process similar to RO, except that ED uses an applied direct current, instead of pressure, to separate ionic contaminants from water. Because water does not physically pass through the membrane in the ED process, particulate matter is not removed. Thus, ED membranes are not technically considered filters. The Electrodialysis Reversal (EDR) process produces water comparable to RO in terms of quality, and may require post-treatment stabilization. The EDR process is often used in treating brackish water to make it suitable for drinking, and tends to be most economical for source water TDS levels in excess of 4,000 mg/L *(Feenstra, et al., 2007).*

2.3 Drawbacks and limitations of defluoridation methods and techniques

Though adsorption depends on the adsorbent and the material it is made from, according to Volesky (2003), extreme variation of pH and temperature lower the adsorptive capacity of the adsorbent. Regeneration is also required after a specific period of time which is dependent on the adsorbent.

Limitations associated with Precipitation-Coprecipitation technologies include large quantity of sludge produced, uncontrolled water pH, difficulty in establishing dose requirement, and high dose requirements for higher fluoride concentrations *(Ayoob et al., 2008).*

The use of anion exchange resins for fluoride removal is not common because of their relatively high costs. The presence of other anions such as chloride and sulphate also presents a major problem when using ion exchange resins for fluoride removal. Since fluoride removal is accompanied by sorption of other anions, the sorption capacity is normally lower than 0.5 mg/L *(Veressinina, et al., 2001).* Regeneration of resin is a problem because it leads to fluoride rich waste, which has to be treated separately before final disposal.

Membrane Processes have the ability to remove all the ions present in water, though some minerals are essential for proper growth. Remineralisation is the required treatment *(Maheshwari, et al., 2006).* Drawbacks to membrane processes include a high-energy requirement associated with operation of high pressure pumps and the complexity of the process (Tetra Chemicals Europe, 2010).

2.4 Clay

Natural clays are abundantly available low-cost natural resources which are nontoxic to ecosystems. Over the recent years, research on the modification of clay to increase their adsorbent capacity to remove other contaminants from drinking water such as fluoride and other metals has been in progress *(Hartman, et al., 1990).*

Clay minerals are generally categorized into the following groups: montmorillonite, smectite, kaolinite, illite, and chlorite. They are widely used because of their high specific surface area, chemical and mechanical stability and low cost (Lin and Juang, 2002).

According to Pinnavaia, et al., 1983, Clays are hydrous aluminosilicates broadly defined as those minerals that make up the colloid fraction of soils, sediments, rocks, and water. They

may be composed of mixtures of fine grained clay minerals and clay-sized crystals of other minerals such as quartz, carbonate, and metal oxides.

Clays play an important role in the environment by acting as natural scavengers of pollutants by taking up cations and anions either through ion exchange or adsorption or both. Clays invariably contain exchangeable cations and anions held to the surface. The prominent cations and anions found on clay surface are Ca^{2+}, Mg^{2+}, H^{+}, K^{+}, NH_4^{+}, Na^{+}, SO_4^{2-}, Cl^{-}, PO_4^{3-}, and NO^{3-}. These ions can be exchanged with other ions relatively easily without affecting the clay mineral structure. Large specific surface area, chemical and mechanical stability, layered structure, high cation exchange capacity (CEC), and so forth have made the clays excellent adsorbent materials (Cadena, 1990).

In this thesis proposal where clay and polymer will fabricate a nanocomposite, it is of paramount importance to understand the morphology that occurs in the polymer silicate nanocomposite, it is important to review the structural details of layered silicate and their properties. The clay to be used in the fabrication of polymer silicate nanocomposites is based on the 2:1 layered structure also known as phyllosilicate *(Zanetti, et al., 2000).* The crystal structure is made up of a layer of aluminium hydroxide octahedral sheet sandwiched between two layers of silicon oxide tetrahedral sheets.

2.4.1 Mukondeni black clay

According to Dacosta, et al., 2013, the presence of smectite in Mukondeni black clay was confirmed by additional XRD analysis after exposing the samples to an ethylene glycol enriched atmosphere.

The most heavily used filler materials in the fabrication of CPNCs are based on the 2:1 layered structure also known as phyllosilicates, of which the most common representative is montmorillonite *(Nguyen, et al., 2005).* Montmorillonite is commonly used in polymer nanocomposite preparation *(Lepoittevin, et al, 2002)*

Mukondeni black clay as being a phyllosilicate was used with a polymer in the synthesis of a CPNC to be used in defluoridation batch experiments. The lower charge densities formed in phyllosicates (Mukondeni black clay as a representative) causes weak electrostatic forces between layers. Also the presence of sodium cations, with high affinity for hydration and exchanging, between the silicate layers make this kind of clay more suitable for swelling, organic modification and exfoliation *(Olad, et al., 2011).*

2.4.2 Modification of clay

Most pristine clays are naturally hydrophilic while most polymers are hydrophobic most polymers are not compatible (miscible) with pristine clays *(Strawhecker, et al., 2000).* The physical mixture of silicate layers and polymer matrix may not form a nanocomposite due to the unmatched chemical affinity between the two. Thus, in order to have a successful development of clay-based nanocomposites, it is necessary to chemically modify a naturally hydrophilic silicate surface to an organophilic one so that it can be compatible with a chosen polymer matrix. To form CPNCs, the immiscibility between the polymer and the hydrophilic clay must be overcome by either modifying the polymer or more frequently and easier, by modifying the clay *(Zhang, et al., 2008).* Generally, this can be done through ion exchange reactions by replacing interlayer cations with quaternary alkyl ammonium or alkylphosphonium cations.

Since polymers are generally organophilic, dispersion of unmodified clays can be difficult to obtain CPNCs since naturally occurring smectite clays are hydrophilic with microcrystalline cellulose being hydrophilic and attracts water molecules due to its functional groups, but since it is in a polymer chain, water does not have the ability to "surround" completely each monomer of the cellulose fiber and dissolve it.

Through clay surface modification, Mukondeni black clay can be made organophilic and therefore compatible with the chosen polymer (cellulose). Lepoittevin, et al (2002), reported modification for polymer-silicate compatibility promoted by an ion-exchange reaction of the silicate interlayer sodium cations with alky ammonium cations. Giannelis et al (1997)'s study highlighted the key role of both the structure of the ammonium used to modify the layered silicates and the dispersion technique wherein several montmorillonites were melt blended to bear either non-functional long alkyl chains or chains terminated by carboxylic acid or hydroxyl groups.

2.5 Polymers

The importance of both natural and synthetic polymers in our lives cannot be overestimated. The desirable properties of these macromolecules, such as tensile strength and flexibility, make them extremely useful both in nature and in the manufacture of products that we use every day.

Polymers are substances made up of recurring structural units, each of which can be regarded as derived from a specific compound called a monomer. The number of monomeric units

usually is large and variable, each sample of a given polymer being characteristically a mixture of molecules with different molecular weights (Ramsden, 2000). The range of molecular weights is sometimes quite narrow, but is more often very broad. The concept of polymers being mixtures of molecules with long chains of atoms connected to one another seems simple and logical today, but was not accepted until the 1930's when the results of the extensive work of H. Staudinger, finally became appreciated. Prior to Staudinger's work, polymers were believed to be colloidal aggregates of small molecules with quite nonspecific chemical structures (Mandelkern, 1972).

There are both naturally occurring polymers such as proteins, starches and cellulose, and synthetic polymers such as polythene, polyvinyl chloride, nylon and Teflon, which are produced commercially on a very large scale and have a wide range of properties and uses (Ramsden, 2000). Polymers have a maximum temperature of 250 ºC and at higher temperatures degradation may occur.

2.5.1 Types of polymers

Polymers can be classified in several different ways i.e. according to their structures, the types of reactions by which they are prepared, their physical properties, or their technological uses

2.5.1.1 Natural and synthetic polymers

Polymers can occur naturally or can be synthesized from their monomers. The polymers used in water treatment can be natural or synthetic, and present high capacity to adsorb on the surface of suspended particles in water (Letterman and Pero, 1990).

It is reported that dissolved Pharmaceuticals were removed by adsorption on some natural and synthetic polymers. Ahmed, et al., 2013, selected Cellulose, chitosan and sodium alginate as natural polymers and epichlorohydrin and urea as synthetic copolymers in removing antibiotics from water. Both types of polymers removed more than 75% of the drug through adsorption. This demonstrates that polymers have adsorptive capabilities and are suitable candidates to be used in adsorption experiments.

2.5.1.2 Thermosetting polymers

According to Treloar (1972), there are three types of solid polymers: elastomers, thermoplastic polymers, and thermosetting polymers. Elastomers are rubbers or rubberlike elastic materials. Thermoplastic polymers are hard at room temperature, but on heating become soft and more or less fluid and can be moulded. Thermosetting polymers can be moulded at room temperature

or above, but when heated more strongly become hard and infusible. Examples are polyethylene, polystyrene and polyvinyl chloride.

2.5.1.3 Polymers formed through Polymerization

During polymerization, monomers link together to form the chain, like a string of pearls. Polymerization usually occurs only in the presence of a catalyst. The units of polymers can be simple or complex. The length of a polymer chain can be long or short. Chemists recognize two main categories of polymers, addition polymers and condensation polymers (Painter and Coleman, 2009).

Addition polymerization occurs with monomers that have double bonds, typically unsaturated carbon molecules. (A saturated compound only has single bonds.) During the reaction, the double bonds open, allowing the monomers to form a long continuous chain. The chemical industry uses addition polymerization widely for creating synthetic polymers, many of which are not biodegradable (Harris, 2003).

Condensation polymerization occurs when monomers with two functional groups react. (A functional group is a distinct group of atoms within a molecule.) Unlike addition polymerization, this type of polymerization involves a smaller molecule being removed. The molecule is often water, which will condense if conditions are right - hence the name.

2.5.2 Polymers used in clay polymer nanocomposites

2.5.3 Cellulose

The structure of cellulose, $(C_6H_{10}O_5)_n$, is the most abundant renewable organic compound. It is primarily found in the cell walls of plants, algae, and bacteria. Cellulose is a polymer composed of 100 to 10,000 monomers of glucose (also called anhydroglucose units) connected by β (1-4) glycosidic bonds (Ghebreselassie, 2013). Most of the properties of cellulose depend on the number of glucose units that form one polymer molecule, that is, the chain length or degree of polymerization.

The simplest structural subunit (the monomer) of cellulose is cellobiose. It is the basic repeating unit in cellulose as each successive glucose unit is rotated by 180◦ around the axis of the polymer backbone chain relative to the last repeated unit (see Figure 1).

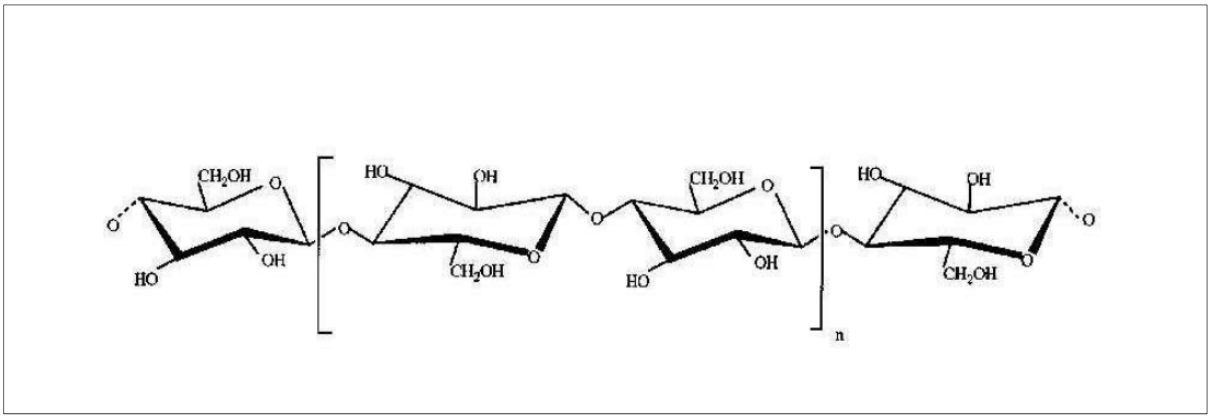

Figure 1: Structural formula of cellulose (Chen, 2014)

Cellobiose is indicated in brackets. Cellulose is tasteless, odourless, and hydrophilic, and insoluble in water, dilute acid, common organic solvents and oils. It is partially soluble in dilute alkali. It is relatively free of organic and non-organic contaminants. It is metabolically inert and has excellent water absorptive, swelling and dispersion properties *(Brown Jr., et al., 1996).* In the interaction with water new pores are generated as the cellulose particles swell, swelling is usually defined as the amount of water contained in the saturated fiber cell wall. Liquids that are able to penetrate into the crystalline regions induce intracrystalline swelling of cellulose (Zeronian, 1985).

Cellulose can be broken down to its simplest forms if treated by strong acids at high temperature. The cellulose polymer has a very rigid chain and complex networks of hydrogen bonds. These characteristics lead cellulose to poor solubility in various organic and inorganic solvents *(Bochek, et al., 2003).* This problem of dissolution hinders the application of cellulose. In spite of its insolubility in various solvents, cellulose is one of the most widely used organic substances and has become a vital commercial raw material (Emerton, 1980).

It's these physiochemical properties that make microcrystalline cellulose a good candidate for fluoride adsorption from aqueous solutions (Weise, 1997). Hydrogen bonds within and between cellulose chains gives the cellulose molecule a stiff and rigid nature. Water molecules can be adsorbed on the cellulose surfaces and bound to the free hydroxyl groups of cellulose chains by hydrogen bonds (Maloney, 2000). Water is held also in pores and gaps between the fibers (Weise, 1997). In addition to the water adsorption to the surfaces, water is also absorbed into the amorphous parts of cellulose *(Stone, et al., 1968).* Microcrystalline cellulose (MCC) is considered the golden excipient for extrusion process, because of its binding and rheological

properties *(Shah et al., 1994).* It can absorb high amounts of water, as it has large surface area and high internal porosity *(Sonanglio et al., 1995).*

2.6 Types of clay polymer nanocomposites

A class of adsorbents currently receiving growing attention is the clay-polymer nanocomposite adsorbent. CPNCs effectively treat water by adsorption and flocculation of both inorganic and organic micropollutants from aqueous solution. Some of these CPNCs also can efficiently remove microorganisms such as *Escherichia coli, Pseudomonas aeruginosa, Staphylococcus aureus* and *Candida albicans* from water (Unuabonah, et al., 2014). Per Schadler, 2004, at the beginning of the last decade, traditional micrometer scale composites reached the limits of properties optimization since to achieve one required property involved the loss of another. Moreover, agglomerates of micrometer-scale fillers can promote macroscopic defects that can lead to breakdown or failure (Schadler, 2004).

In a composite, one phase is continues and is called matrix, while the other is filler material which make the dispread phase *(Sun et al., 2011).*

CPNCs are of two different types. In general, the degree of dispersion of the clay platelets into the polymer matrix determines the structure of nanocomposites. Depending on the interaction between the clay and the polymer matrix, the two main idealized types of clay polymer morphologies that can be obtained are intercalated and exfoliated *(Ali, et al., 2011).*

The intercalated structure results from penetration of a single polymer chain into the galleries between the silicate layers, resulting in formation of alternate layers of polymer and inorganic layers, insertion of polymer chains into a layered silicate structure occurs in a crystallographically regular fashion, with a repeat distance of few nanometers, regardless of polymer to clay ratio (see figure 2) *(Masenelli-Varlot, et al., 2002).*

An exfoliated structure results when the individual silicate layers are completely separated and dispersed randomly in a polymer matrix. Usually exfoliated nanocomposites are preferred because they provide the best property improvements (see figure 2) *(Masenelli-Varlot, et al., 2002).* With exfoliated nanocomposites, individual silicate layers are separated in the polymer matrix by average distances that depend only on the clay loading *(Suprakas, et al., 2003).*

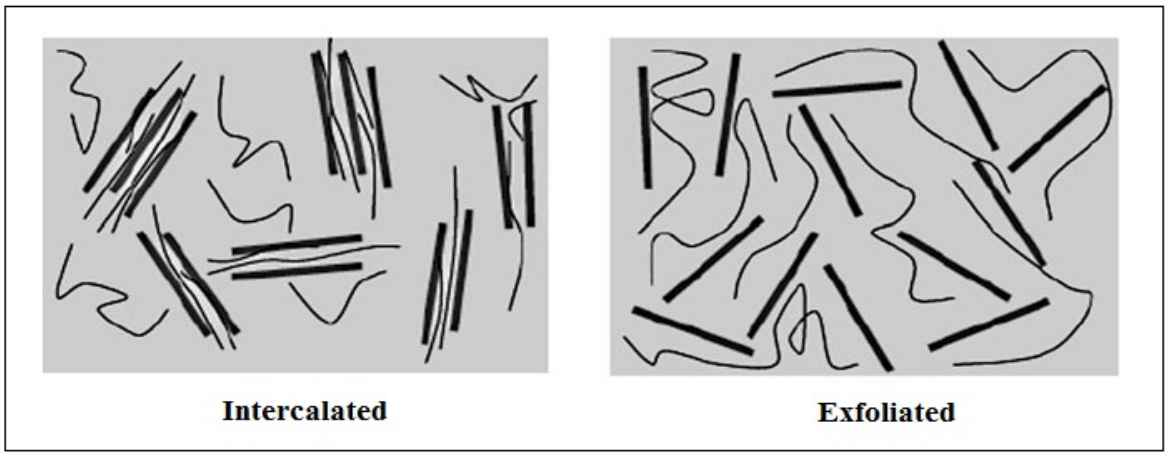

Figure 2: Schematic illustrations of two types of polymer-layered silicate morphologies: (left intercalated and (right) exfoliated (sinha-Ray and Okamoto, 2003).

The interface plays a central role on the nanocomposites final properties. Taking the example by kickelbick, if a cube of atoms packing 16 x 16 x 16 atoms, this contains an overall number of 4096 atoms from which 1352 are located on surface (33% surface atoms) *(Kickelbick, et al., 2007).* However, if the cube is divided into eight equal parts the overall atoms number is the same but the number of atoms at the surface increase to 2368 (58% surface atoms), repeating the process we reached to 3584 surface atoms (88% surface atoms).

Generally three ways are used to disperse inorganic nanoparticles into polymer matrices. The first uses the top-down methodology, which consists in the direct mixing of the filler into a polymeric matrix in solution or in melt. The second is based on in-situ polymerization in the presence of the nanoparticles previous obtained or in-situ synthesis of inorganic nanoparticles in the presence of polymer. The last one, inorganic and organic components are both formed in-situ *(Oliveira, et al., 2012).* These two last methods are defined as bottom-up methodologies.

The efficiency of organic modification by ion exchange process in the increasing of basal spacing and consequently the exfoliation of clay and formation of stable nanocomposite systems depends also on the surface charge of clay layers. The surface charge density of clay layers depends on the clay nature and its preparation conditions *(Olad, et al., 2011).*

Intense studied applications of CPNCs are the removal of inorganic micropollutants from aqueous solutions. Clay-polymethoxyethylacrylamide (PMEA) nanocomposites prepared by Sölener et al. (2008) was used to removed Pb(□) from aqueous solution with a very high adsorption capacity of 81.02mg/g. Anirudhan and Ramachandran (2008) prepared an

organobentonite ammoxidated polyacrylonitrile (OBent-PAN) nanocomposite with a pH_{PZC} of 6.3 and adsorption capacity of 77.43, 65.4 and 52.61 mg/g for the removal of Cu(□), Zn(□) and Cd(□), respectively from aqueous solution.

With current reviews highlighting that CPNCs have been used successfully for the removal through adsorption of micropollutants, these very same CPNCs can prove to be suitable potential candidates for the removal of fluoride from groundwater through adsorption.

2.7 Methods used for clay polymer nanocomposite synthesis

In-situ polymerisation and melt intercalation are the most common methods to fabricate CPNCs. The direct intercalation behaviour of a molten polymer into an organically modified clay was first observed by Vaia et al. employing polystyrene and an alkyl-ammonium modified montmorillonite *(Vaia, et al., 1997).*

The structures of polymer clay nanocomposites are classified according to the level of intercalation and exfoliation of polymer chains into the clay galleries. Various parameters including clay nature, organic modifier, polymer matrix and preparation method are affective on the intercalation and exfoliation level *(Oliveira, et al., 2013)*. Therefore depending on the nature and properties of clay and polymer as well as preparation methodology of the nanocomposite, different composites micro structures can be obtained.

2.7.1 In-situ intercalation

In the in situ polymerization method, the monomer is used directly as a solubilizing agent for swelling the layered silicate. Subsequent polymerization takes place after combining the silicate layers and monomer, thus allowing formation of polymer chains between the intercalated sheets *(Zanetti, et al., 2000).*

Nanocomposites can be prepared by in-situ synthesis of inorganic particles or by dispersion of fillers in a polymeric matrix *(Kickelbick, et al., 2007).* A correct selection of the preparation technic is critical to obtain nanomaterials with suitable properties *(Ruiz-Hitzky, et al., 2011)*. The synthesis of polymers nanocomposites usually applies bottom-up or top-down methodologies. In the bottom-up approach, precursors are used to construct and grow, from the nanometric level, well organised structures.

2.7.2 Intercalation from solution

This second method involves intercalation of polymer from solution. This method requires a suitable solvent that can both solubilize the polymer and swell the silicate layers. When the layered silicate is dispersed within a solution of the polymer, the polymer chains intercalate and displace the solvent within the gallery of the silicate. A CPNC is obtained upon the removal of the solvent, either by solvent evaporation or polymer precipitation *(Jimenez, et al., 1997).*

2.7.3 Melt intercalation

The last method, melt intercalation, does not require the use of a compatible solvent or suitable monomer. In this method, a polymer and layered silicate mixture is heated under either batch or continuous shear (in an extruder) above the softening point of the polymer. During the heating process, polymer chains diffuse from the molten polymer into the silicate galleries to form either intercalated or exfoliated depending on the degree of penetration *(Zanetti, et al., 2000).*

Depending on the nature of the modified clay, polymer and instrument to be used, a binder may be required within the composite and later incinerated. One important characteristic of the binder is its ability to be effectively and evenly distributed through the interparticulate voids in a compound *(Pandey, at al., 2017).*

This method is an effective technique for the preparation of CPNCs *(Kornmann et al., 2001).* Clays are organically modified and the clay polymer composite are surface modified with a binder for more polar functional groups to enhance their compatibility and therefore promote the exfoliation process. Melt intercalation has many advantages for the preparation of nanocomposites and is a popular method for industry *(Ray et al., 2003).*

The melt intercalation method has great advantages over either polymerization intercalation or polymer solution intercalation. Firstly, this method is environmentally benign due to the absence of organic solvents. Secondly, it is compatible with current industrial mixing and manufacturing techniques. Nano composites can, therefore, be manufacture using industrial processes, such as extrusion and injection molding *(Kojima, et al, 1994),* methods such as extrusion and injection molding are used for dispersion of clay layers within the polymer matrix.

2.8 Drawbacks and limitations of methods for clay polymer nanocomposite synthesis

The drawbacks in the above mentioned methods are the requirement of suitable monomer/solvent or polymer solvent pairs for in-situ intercalation polymerization and intercalation of polymer from solution and the high costs associated with the solvents, their disposal, and their impact on the environment. There is a lack of information about their fate and behaviour in the environment as well as the potential health and environmental risk (Helland, 2008).

Very high/low melting point have been consider as a disadvantage for the melt intercalation method for various polymers that a subjected to shear (Scallan and Carles, 1972).

2.9 Characterization techniques

The nanocomposite structure, namely, intercalated or exfoliated, may be identified by monitoring the position, shape, and intensity of the basal reflections from the distributed silicate layers. X-ray Diffraction (XRD) can offer a convenient method to determine the interlayer spacing of the silicate layers in the original layered silicates and in intercalated nanocomposites *(Bridley, et al., 1980).*

To supplement the deficiencies of XRD, Transmission electron microscopy (TEM) can be used. TEM allows a qualitative understanding of the internal structure, spatial distribution of the various phases, and views of the defect structure through direct visualization *(Roe, et al., 2000).* Together, TEM and XRD are essential tools for evaluating nanocomposite structure *(Bridley, et al., 1980).* TEM is time consuming and gives qualitative information on selected regions of the sample, whereas low-angle peaks in XRD allow quantification of changes in layer spacing.

Scanning Electron Microscopy (SEM) provides nanoparticle morphology and estimates the sample composition through EDS. SEM creates an image of the sample by scanning its surface with a low-energy beam of electrons (typically from 1 to 30 ke V) achieving resolutions in the low nanometre range (Anonymous Food, 2011).

Fourier Transform Infrared Spectroscopy (FTIR) offers quantitative and qualitative analysis for organic and inorganic samples. FTIR is an effective analytical instrument for detecting functional groups and characterizing covalent bonding information in CPNCs (Lendl, 2015).

2.10 Equilibrium adsorption models

An adsorption isotherm is one of the most significant tools to predict the adsorption capacity of the adsorbent and the adsorption mechanism *(Zhang et al., 2011)*. The distribution of fluoride between the liquid and solid phases can be expressed by the Langmuir and Freundlich equations in the adsorption process *(Sun et al., 2011).*

2.10.1 Langmuir Adsorption isotherms

Langmuir adsorption isotherm is the most applicable isotherm commonly applied in solid/liquid system to describe saturated monolayers sorption *(Sun et al., 2011).* It assumes that the adsorbent surface is uniform, i.e., all the adsorption sites are equivalent and adsorption molecules do not interact *(Zhang et al., 2011).* The linear equation of Langmuir adsorption is expressed as follows:

$$\frac{1}{qe} = \frac{1}{q_o b} \times \frac{1}{C_e} + \frac{1}{q_o} \quad \text{..... (1)}$$

Where: C_e is the equilibrium concentration (mg/L)

q_e is the adsorption capacity (mg/L)

q_o is theortical maximum adsorption capacity

b is the Langmuir constant related to enthalpy of adsorption

q_o and b are determined from the slope and intercept of the plot of $\frac{1}{qe}$ vs $\frac{1}{C_e}$

In order to predict the adsorption efficiency of the process, the dimensionless equilibrium parameter (R_L) will be calculated using the following equation:

$$R_L = \frac{1}{1+bc_o} \quad \text{..... (2)}$$

Where: C_o is the initial concentration of adsorbate (mg/L).

b is the Langmuir isotherm constant

If R_L value is between 0 and 1 the adsorption is favourable.

2.10.2 Freundlich adsorption isotherm

Freundlich adsorption model is empirical model which is an indicative of the surface heterogeneity of adsorbent *(Kamble et al., 2009).* It is expressed by the following equation:

$$\log Q_e = \log kf + \frac{1}{n}\log Ce \quad \text{..... (3)}$$

Where: *Ce* = equilibrium concentration (mg/L)

Qe = amount adsorbed at equilibrium (mg/g)

Kf = freundlich constant related to adsorption capacity

n = is the adsorption intensity

The value of kf and n are obtained from the slope and intercepts of linear plot of log Q_e vs log C_e.

2.11 Adsorption kinetics

In order to understand the adsorption mechanisms, the adsorption kinetic isotherms were described using reaction based models which are pseudo first order and pseudo second order models *(Thakre et al., 2010).* The pseudo first order and Pseudo second order models are generally expressed as follows:

Pseudo first order:

$$\log(q_e - q_t) = \log(q_e) - \frac{k_{ad}t}{2.303} \quad \text{..... (4)}$$

Where q_e and q_t (both in mg/g) are the amount adsorbed per unit mass at a time, t (in min). And K_{ad} is the rate constant ($g.mg^{-1}/min$).

Pseudo second order:

$$\frac{t}{q_t} = \frac{1}{K_{2ads}q_e^2} + \frac{1}{q_e}t \quad \text{..... (5)}$$

Where: q_t is the amount of fluoride adsorbed at time (mg/g). q_e is the amount of fluoride adsorbed at equilibrium (mg/g). K_{2ads} is the pseudo second order rate constant ($g.mg^{-1}/min$) and *t* is time (min). These kinetic models will give the understanding of rate at which the adsorption is taking place.

This chapter reviewed literature related to fluoride, its health hazards, occurrence of fluoride in groundwater, methods of removing fluoride from groundwater, polymers and their use in nanocomposites, clay soils and their defluoridation capabilities and the use of nanocomposites in water purification. It is evident in the literature review that nanocomposites are receiving growing attention as effective adsorbents. This study adds through batch adsorption experiments, knowledge of clay polymer nanocomposites as adsorbents with specific consideration to defluoridation of groundwater.

CHAPTER THREE

Materials and Methods

3.1. Reagents and sampling

The polymer used in this work was microcrystalline cellulose in white powder form with a Bulk density of 0.29 g/ml, Loss on drying: 3.7 %, Residue on Ignition: 0.003 %, and Mesh size of 0.00 % >60 mesh. Microcrystalline cellulose was purchased from Monitoring & Control Laboratories (PTY) LTD in South Africa and was used as received.

Mukondeni black clay was collected from Mukondeni Village in Vhembe district, Limpopo Province, South Africa.

Clay surface modification was done using clear colourless liquid Ammonium hydroxide, 28 % NH3 with an aqueous acid-base titration of 33.2 %. Ammonium hydroxide was purchased from Rochelle Chemicals & Lab Equipment cc, South Africa.

Ethylene glycol (99.96 %) was used as a binder and was purchased from Rochelle Chemicals & Lab Equipment cc, South Africa.

High fluoride groundwater was collected from a community borehole in Siloam village, Nzhelele in Vhembe district, Limpopo Province, South Africa.

3.2 Preparation of Mukondeni black clay

The raw Mukondeni black clay sample was washed with ultra-pure water repeatedly to remove impurities. The Mukondeni black clay sample was further purified by adding 60 g in 600 mL ultra-pure water containing 2.5M HCL, the solution was stirred at 360 rpm for 3 hours at 60 °C using a magnetic stirrer. The purified clay was then separated by filtration (whatman No. 42 filter paper). The filter cake was washed with distilled water and dried at 105 °C overnight. The sample was milled into fine powder using a Retsch RS 200 miller.

3.3 Modification of Mukondeni black clay

Hydrophilic nanoparticles and hydrophobic polymers are not compatible, which results in poor interfacial adhesion, consequently bad dispersion and poor properties *(Rong, et al,. 2001).* Modification of clay layers with hydrophobic agents is necessary in order to render the clay layers more compatible with polymer chains *(Ali, et al., 2011).* The ion exchange process is carried out in aqueous solution with hydrated inter silicate layers. The affinity of Alkyl

Ammonium cations to hydration promotes the ion exchange process and increases the efficiency of organic modification of clay layers.

Mukondeni black clay was modified with ammonium hydroxide, by adding amounts of surfactant equivalent to the cation exchange capacity (CEC) of the Mukondeni black clay. The surfactant, Ammonium hydroxide, was dissolved in 500 mL of distilled water, 60 g of Mukondeni black clay was added and stirred with a digital magnetic hot plate stirrer for 6 hours at 360 rpm at a temperature of 60 °C. Mukondeni black clay was separated from the solution by filtration and washed with distilled water. The obtained clay was further washed repeatedly then dried at 105 °C overnight. The dried clay was milled and stored in labelled polyethylene plastic bags for further use in the synthesis of a CPNC.

This clay modification method has been used before and was adopted from Singla, et al, 2012, Clay modification by the use of organic cations.

3.4 Method used for the synthesis of clay polymer nanocomposites

3.4.1 Melt intercalation

The instrument used in melt intercalation was HAAKE PolyLab OS RheoDrive 4 Thermo. This is a state-of-the-art measuring mixer and extruder system that provides process-relevant data i.e. melt behaviour, influence of additives, temperature stability, shear and melt viscosity. Furthermore, this measuring mixer and extruder system supports modelling activities such as melt mixing polymers with additives using different L/D ratios to optimize extrusion or mixing in respect to temperature and shear. Specifications for synthesizing the CPNC in this work using the HAAKE PolyLab OS RheoDrive4 Thermo were Twin Screw rotation 60 rpm at 220 °C for 10 minutes for all 4 Samples (clay and cellulose) using 50 g per sample

A key factor in the clay-polymer interaction is the affinity polymer segments have for the silicate surface. Melt intercalation method was used for the synthesis of CPNCs. Melt intercalation process was undertaken as follows. Various ratios of clay to polymer (1:1, 1:2, 1:3 and 1:4) were weighed and manually mixed in a poly ethylene plastic bag to obtain modified clay and microcrystalline cellulose blend. 10 mL of a melt able binder, Poly (ethylene glycol) was added to the various ratios mixture of clay and cellulose. One important characteristic of the binder is its ability to be effectively and evenly distributed through the interparticulate voids in a compound. The mixture was oven vacuumed at 108 °C for the removal of moisture then cooled before being inserted into a twin screw Rheomixer. The

Rheomixer ran for 10 minutes at 220 °C for all 4 ratios. This method has become the mainstream for the fabrication of CPNCs in recent years because it is simple, economical, and environmentally friendly (Vaia, et al., 2002).

3.5 Physicochemical and mineralogical characterization

3.5.1 Thermogravimetric analysis

The volume fraction of the two main constituents of the CPNCs, Mukondeni black clay and microcrystalline cellulose, was determined using a Thermogravimetric Analyzer (TGA), TGA Q500 V20. Samples were heated at a temperature rate of 10 °C/min to a final temperature of 1000 °C while being purged with oxygen at a flow rate of 20 mL/min. Sample weight was recorded as a function of temperature. Mukondeni black clay and microcrystalline cellulose volume fraction was determined by measuring the loss in sample weight with temperature.

3.5.2 X-ray diffraction (XRD) analysis

The mineralogical analysis of Mukondeni clay and cellulose was carried out using the Bruker LynxEye XE Detector X-ray diffraction Instrument. Measurements used during analysis were 40 kV Tube voltage, 35 mA Tube current, Variable slits: V20 variable slit at 2ϑ Range: 6 to 90 (angles in degrees) with Increment Δ2ϑ: (0.034). Time: 0.5 sec/step.

3.5.3 X-ray Fluorescence (XRF) analysis

The CPNC samples were roasted at 1000°° C to determine Loss On Ignition (LOI), 1g Roasted sample was then placed together with 6g of Li2B4O7 into a Pt/Au crucible and fused. The ARL Perform'X Sequential XRF was used for the analyses. Analyses were executed using the Quantas software. The software analyse for all elements in the periodic table between Na and U, but only elements found above the detection limits were reported. The results were also monitored and filtered to eliminate the presence of some of the flux, wetting and oxidising agent elements.

3.5.4 Brunauer-Emmett-Teller (BET) analysis

The TriStar II 3020 V1.02 instrument was used to measure the specific surface area of the clay polymer nanocomposites, including the pore size distribution. 1 g of CPNC was used with a sample density of 1000 g/cm^3.

3.5.5 Scanning Electron Microscopy (SEM) analysis

Clay surface morphology was determined using Scanning electron microscopy (SEM) using the Leo Nova NanoSEM 450 instrument. Magnification was varied from 10 000x and 20 000x.

3.5.6 Fourier Transform Infrared Spectroscopy (FTIR) analysis

Fourier Transform-Infrared Spectroscopy (FTIR) was used to identify organic and polymeric material using the ALPHA, FTIR Instrument. There instrument was used at a spectral range of 8000 cm^{-1} – 10 cm^{-1}.

3.5.7 Cation Exchange capacity (CEC)

Cation exchange capacity is a measure of the number of exchangeable sites within soil for cations. The method used for CEC analysis was the ammonium acetate method, the solutions were buffered at a pH of 7. Ammonium is a good ion to choose for replacing other cations. 10 mg of Mukondeni black clay was poured into a 100 mL polyethylene plastic bottle, the polyethylene plastic bottle was topped up with a solution of 1 mol ammonium acetate and shaken for 30 minutes at 250 rpm using the Stuart reciprocating shaker. The solution was than vacuum filtered using whatman 42 filter paper. The collecting filtrate was disposed, 40 mL of 1 mol potassium chloride (KCL) solution was poured into the collected filter cake. The potassium ions displace all the ammonium ions that were currently on the site hence ammonium can be measured. The filtrate was collected and analysed for potassium.

3.6 Optimizing conditions for clay polymer nanocomposites

3.6.1 Preparation of F^- stock solution

1000 mg/L fluoride solution was prepared by dissolving 2.21g of NaF salt in ultra-pure water. 10 mL was extracted from the 1000 mg/L solution into a 1000 mL volumetric flask that was topped-up to the mark using ultra-pure water to make a 10 mg/L fluoride solution.

3.6.2 Effect of contact time

To evaluate the effect of contact time in the optimization of clay polymer nanocomposites, 4 samples each in polyethylene plastic bottles, were topped up to make a fluoride solution of 10 mg/L. 1g of different ratios (1:1, 1:2, 1:3 and 1:4) of CPNC was added into each plastic bottles. The mixture was then shaken for 1, 5, 10, 15, 30, 60, 120, and 360 minutes at 250 rpm using a table shaker. pH, Temperature, and EC was measured by the CRISON multimeter probe (model MM40) before and after stirring. Fluoride was measured by the CRISON multimeter probe.

3.6.3 Effect of adsorbent dose

To evaluate the effect of adsorbent dose on fluoride removal 16 samples of 10 mg/L fluoride solution were topped into 16 polyethylene plastic bottles. 4 different masses (0.05 g, 0.1 g, 0.5 g and 1 g) of CPNC were weighed within each ratio (1:1, 1:2, 1:3 and 1:4) of CPNC added into each plastic bottles. The mixture was then shaken for 1, 5, 10, 15, 30, 60, 120, and 360 minutes using a table shaker at 250 rpm. pH, Temperature, and EC was measured by the CRISON multimeter probe (model MM40) before and after stirring. Fluoride was measured by the CRISON multimeter probe.

3.6.4 Effect of pH

To evaluate the effect of pH 20 samples of 10 mg/L fluoride solution were topped into 20 polyethylene plastic bottles. The pH was adjusted using 0.1 M HCL and 0.1 M NaOH to 2, 5, 7, 9 and 12. 0.05 g, 0.1 g, 0.5 g and 1 g of CPNC of different ratios (1:1, 1:2, 1:3 and 1:4) was added into each plastic bottles. The mixture was then shaken for 30 minutes using a table shaker. pH, Temperature, and EC was measured by the CRISON multimeter probe (model MM40) before and after stirring. Fluoride was measured by the CRISON multimeter probe.

3.6.5 Effect of adsorbate dose

To evaluate the effect of adsorbate dose 16 samples made up of 4 samples of 5 mg/L fluoride solution, 4 samples of 10 mg/L fluoride solution, 4 samples of 20 mg/L fluoride solution and 4 samples of 50 mg/L fluoride solution were prepared. 1 g of CPNC 1:1, 1:2, 1:3 and 1:4 were added into the varied adsorbate dose samples in polyethylene plastic bottles. The mixture was then shaken for 30 minutes using a table shaker at 250 rpm. pH, Temperature, and EC was measured by the CRISON multimeter probe (model MM40) before and after stirring. Fluoride was measured by the CRISON multimeter probe.

3.7 Defluoridation of Siloam borehole water using clay polymer nanocomposites

Groundwater as collected from a community borehole in Silom village Nzhelele in Limpopo province. Defluoridation experiments were carried out under optimized condition. The concentration of F^- in the groundwater was measured before and after defluoridation by the nanocomposites using the CRISON multimeter probe.

3.8 Calculation of percent of F^- removed by clay polymer nanocomposites

The percent of removal by the clay polymer nanocomposites was determined by the following equation:

$$\% \text{ Removed} = \left(\frac{Co - Ce}{Co}\right) \times 100 \quad \ldots\ldots (6)$$

Where: Co is the initial fluoride ion concentration and Ce is equilibrium fluoride concentration

3.9 Regeneration of clay polymer nanocomposites

Regeneration of the adsorbent was carried out as follows: 5 g of fluoride loaded clay was agitated with 100 mL of 0.1 M NaOH for 1 hour on a table shaker. After agitation, the adsorbent was filtered through a 0.45 µm pore membrane filter and the filtrate was diluted to 100mL and then analysed for desorbed fluoride. The collected adsorbent was then re-used for three successive defluoridation cycles.

CHAPTER FOUR

Results and Discussions

4.1 Physicochemical and mineralogical characterisation

Mineralogical and chemical composition analysis for all 4 CPNC samples was done using X-ray diffraction (XRD) to determine the mineralogical composition and crystallinity of the cellulose within the nanocomposites. X-ray fluorescence (XRF) was used for elemental chemical composition analysis. Scanning electron microscope (SEM) was used for image morphology, Fourier Transform Infrared Spectroscopy (FTIR) for detecting functional groups and Brunauer-Emmett-Teller (BET) for analysing the specific surface area of the CPNC. Thermogravimetric analysis (TGA) for thermal analysis in changes in physical and chemical properties of CPNC as a function of temperature (with constant heating rate/or constant mass loss) was done using the TGA Q500 V20 instrument.

4.1.1 Thermogravimetric (TGA) analysis

Analysis of thermal changes on Mukondeni black clay was done and thermal decomposition of the clay can be observed in figure 3a below.

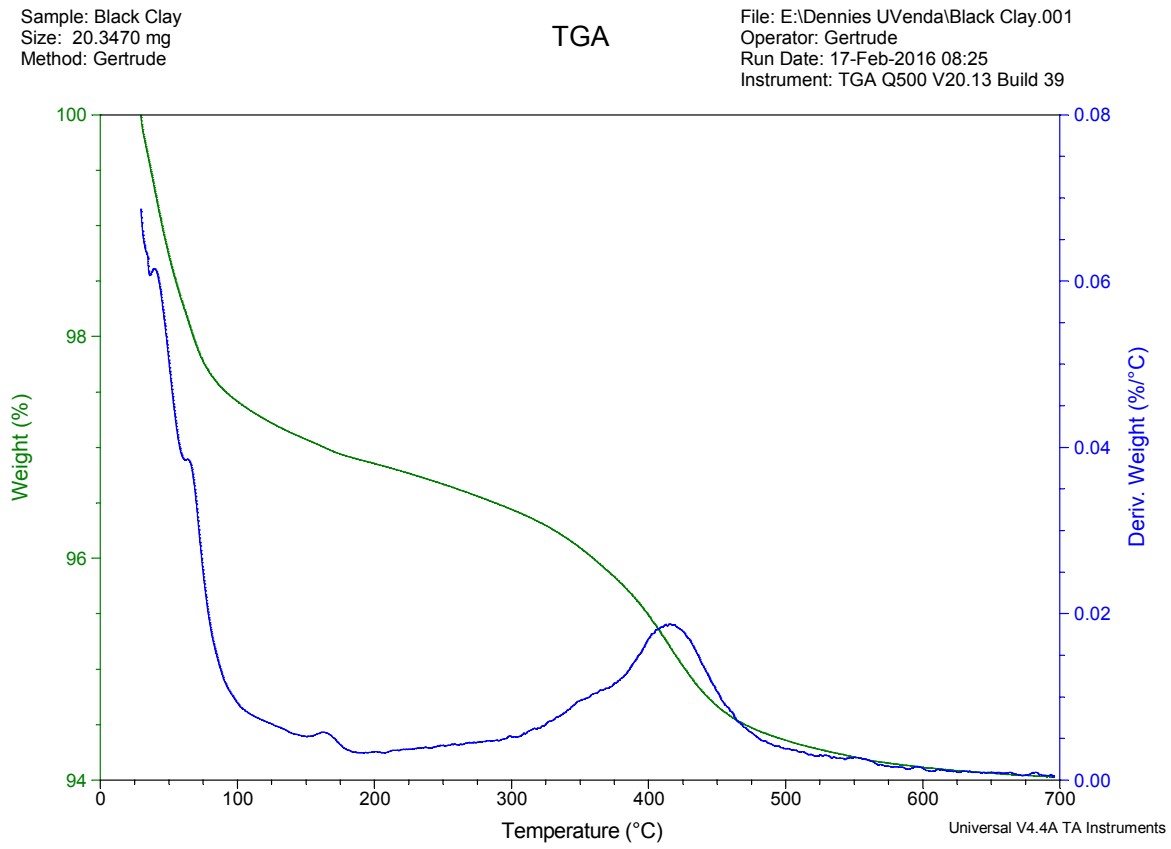

Figure 3a: TGA curves of Mukondeni Black clay

TGA curves of Mukondeni black clay are shown in Figure 3a. It can be observed that the TGA analysis of Mukondeni black clay has two mass loss steps: between 25 °C and 75 °C, at 350 °C and 500 °C. These mass loss steps are attributed to desorption of moisture from the clay, dehydration of the hydrated cation in the interlayer and the dehydroxylation of smectite respectively.

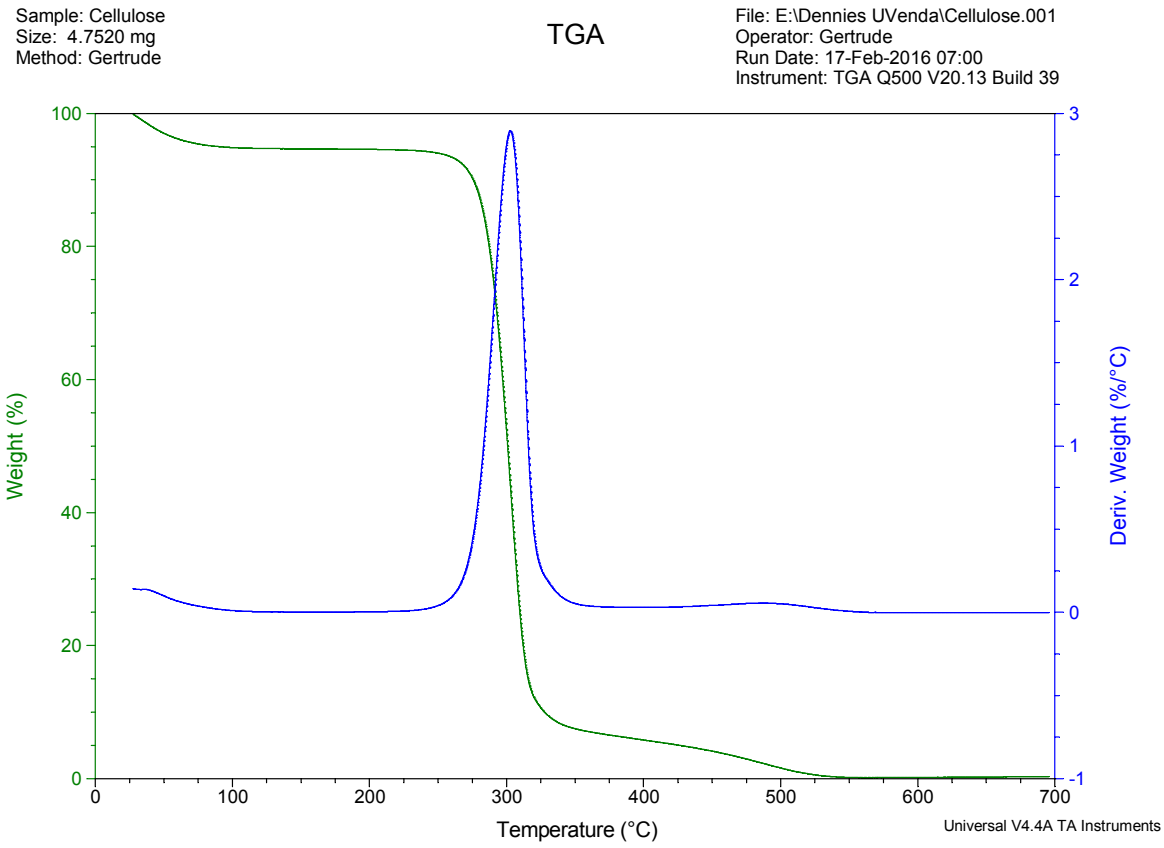

Figure 3b: TGA curves of microcrystalline cellulose

TGA curves of microcrystalline cellulose are shown in Figure 3b. Thermal decomposition of microcrystalline cellulose occurred in one stage with a maximum decomposition rate at 271 °C. 100 % mass loss occurred at 537 °C. Melting of the cellulose occurred at 255 °C. Very high/low melting point have been considered as a disadvantage for various polymers that are subjected to shear (Scallan and Carles, 1972).

Modification of natural clay is therefore necessary to make the clay more compatible with the chosen polymer. A binder to melt the two materials together is also necessary to allow for the melt intercalation method to occur.

4.1.2 X-ray diffraction (XRD) analysis

Mukondeni clay has been successfully modified using organic cationic surfactants. The XRD results show intercalation of the organic cations between the clay mineral layers. Microcrystalline cellulose is a polysaccharide made of D-glucose molecules linked together by glycosidic bonds, its fatty acidic characteristics makes it successful in increasing basal spacing between the clay platelets. Hence basal spacing is also increased by using fatty acid with long hydrophobic chains during clay modification with ammonium hydroxide.

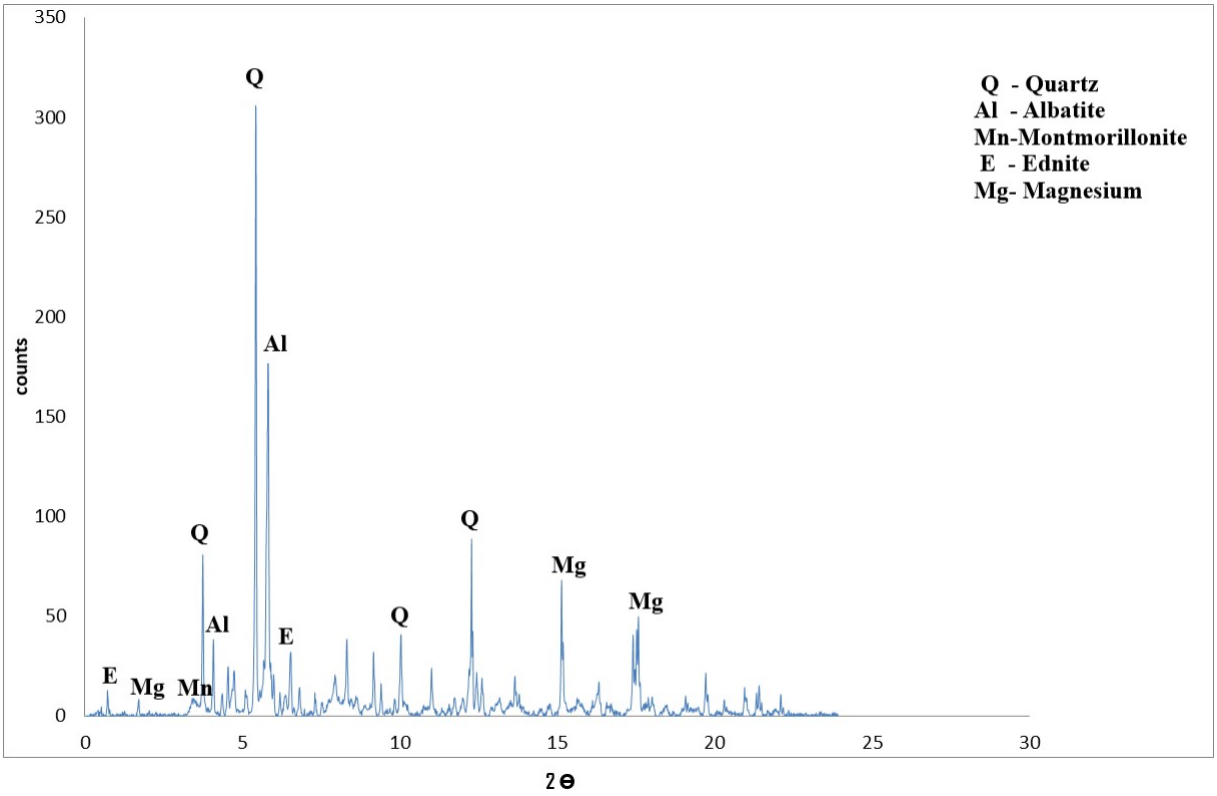

Figure 4: XRD spectra of Mukondeni black clay

XRD analyses were carried out to identify the mineral phase structure of Mukondeni black clay. As shown in figure 4, the clay is mainly characterized of Quartz, Albatite, Montmorillonite, Ednite and Magnesium. The Quantitative results further confirms the presence of smectite (60.34 %) as the major mineral and the presence of quartz (20.21 %) and plagioclase (20.39 %) as minor minerals constituting Mukondeni black clay.

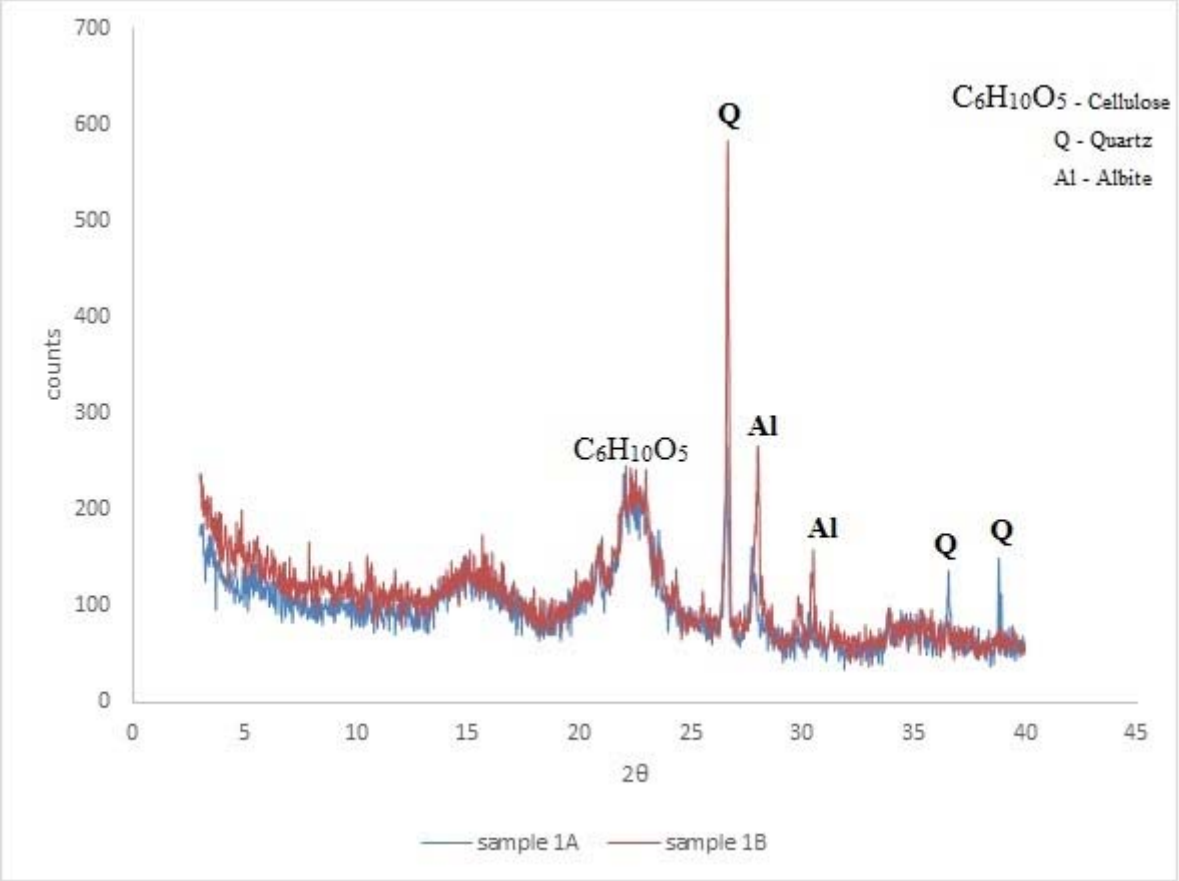

Figure 5a: XRD spectra of CPNC sample 1 (1:1 clay to polymer)

X-ray diffraction was used to determine the changes in the mineral phase structure and the surface properties of the synthesized CPNC.

Incinerating the poly ethylene glycol as a binder in the mixture between cellulose and clay the XRD peaks for the resultant CPNC shows the gradation due to residual water desorption, dehydration, followed by decomposition of the organic modifier. These organically modified montmorillonites have potential utility in the preparation of polymer nanocomposites and in other applications. The organoclays prepared in this study can be used to prepare nanocomposites with polar polymers in order to render good level of dispersion, improved mechanical and other properties. As shown in figure 5a, CPNC 1:1 is mainly characterized of cellulose, Quartz and Albatite as the major minerals with traces of Montmorillonite, Ednite and Magnesium as minor minerals constituting CPNC 1:1.

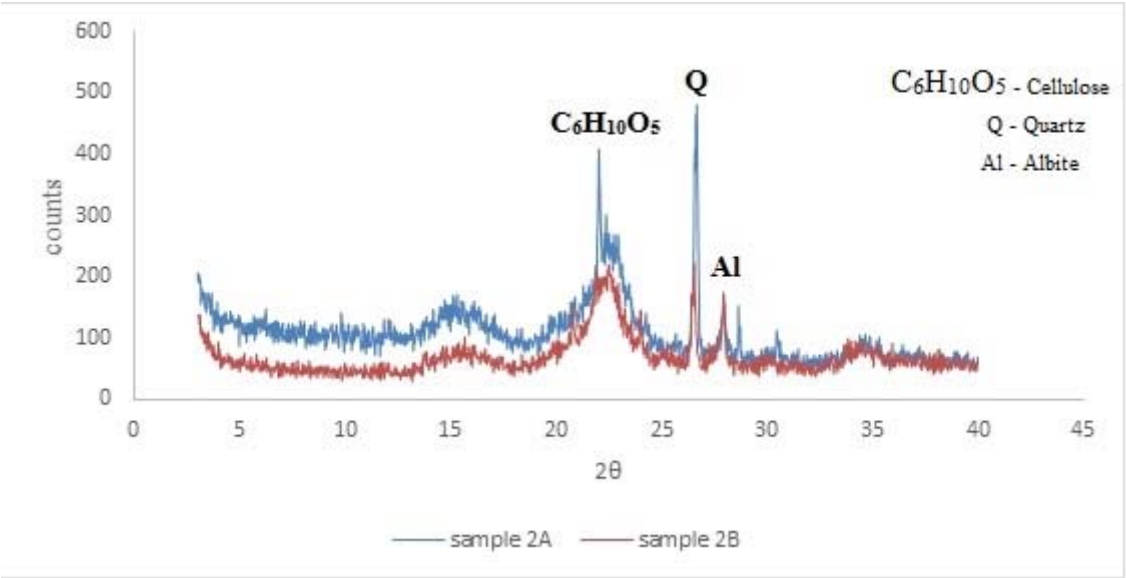

Figure 5b: XRD spectra of CPNC sample 2 (1:2 clay to polymer)

Our XRD measurements showed that the original smectite Mukondeni clay is mainly composed of amorphous phase and contains less than 10% crystal phase present in the form of quartz. Unlike Mukondeni clay that was more than 70% amorphous phase of total mass of the clays, it is evident from figure 5b that CPNC 1:2 is becoming partly amorphous and partly crystalline. Our XRD patterns of CPNC 1:2 showed that a minor change of crystal phase was found in the CPNC activated through melt intercalation by either microcrystalline cellulose as the polymer or using poly ethylene glycol as a binder at a temperature of 220 °C.

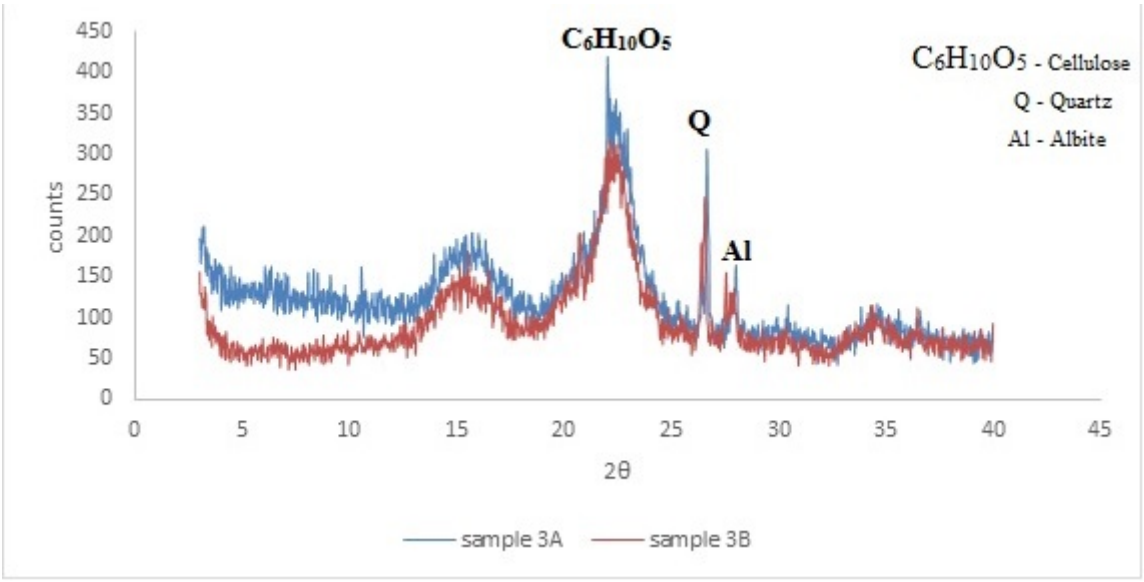

Figure 5c: XRD spectra of CPNC sample 3 (1:3 clay to polymer)

1:3 CPNC further shows in figure 5c the transformation of the CPNC assuming less content of Mukondeni clay constituent (such as Montmorillonite, Ednite and Magnesium which are present in Mukondeni clay as seen in Figure 4) to more cellulose content to give the desired characteristics of the CPNC moreover ordinary composites.

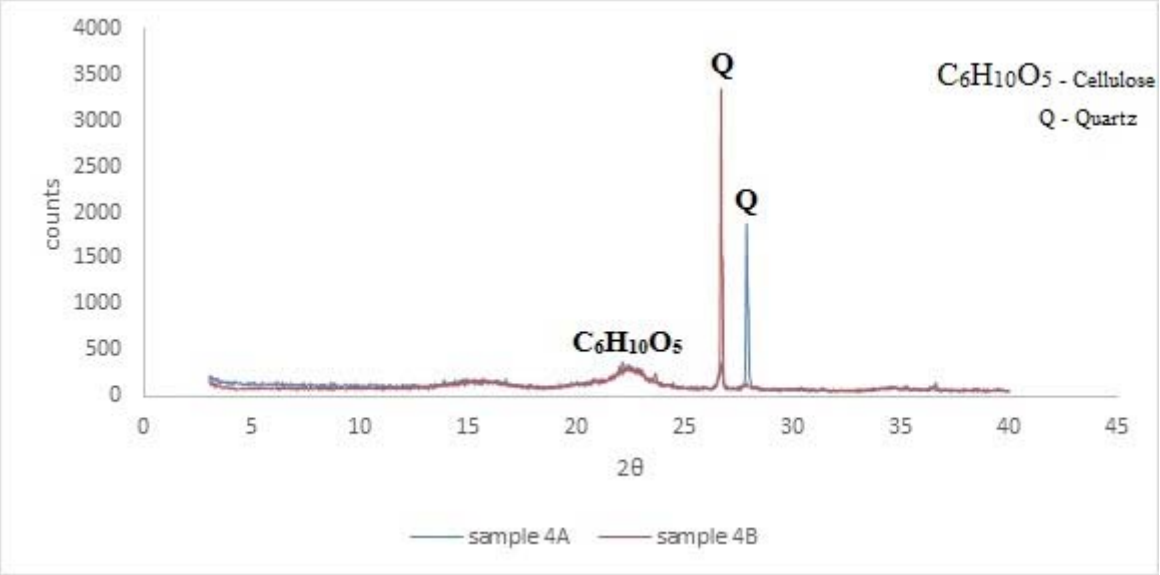

Figure 5d: XRD spectra of CPNC sample 4 (1:4 clay to polymer)

Through exfoliation, the structure of 1:4 CPNC shown above in figure 5d is partially crystalline and partially amorphous as a result of the glycol acting as a binder and stabilizer and the incorporation of microcrystalline cellulose in an increased quantity (1:4 clay to cellulose) as compared to figure 5a (1:1 CPNC), figure 5b (1:2 CPNC) and figure 5c (1:3 CPNC). The XRD above contains both amorphous and polycrystalline mineral structure, this combination gives it the qualities necessary to act as an adsorbent and emulsifying agent. The composites shown in figure 5a, 5b, 5c and 5d demonstrates peaks around 23 and 27 2θ due to cellulose and silicate layers respectively. No further peaks were expected in the spectrum, the lack of peaks for the composite material demonstrates the incineration of the binder and that the composite is a true nanocomposite with the polymer completely intercalated with the exfoliated clay (Delhom, et al., 2009).

4.1.3 X-ray fluorescence (XRF) analysis

Table 4a, 4b, 4c and 4d presents the major elemental composition of CPNC of different ratios of clay to polymer. The analysis reveals that silica (SiO_2) is not the main component of the CPNC as it is averaging 23.87% followed by Al_2O_3 with an average of 5.34%. functional groups of cellulose that are least detected by XRF make up the bulk material of the CPNC as

they increase in ration of clay to cellulose. High concentration of SiO_2 and Al_2O_3 reveal that the CPNC is partially an alumino-silicate material. A decrease in silica content can be observed with an increase in cellulose within the CPNC.

Table 4: Physicochemical properties of clay to polymer nanocomposites.

Parameter	**% composition**			
	1:1	**1:2**	**1:3**	**1:4**
Al2O3	5.34	4	2.67	1.86
CaO	0.99	0.68	0.68	0.46
S	< LOD	< LOD	< LOD	< LOD
Cr2O3	0.06	0.06	0.05	0.04
Fe2O3	2.70	2.13	2.70	1.43
K2O	0.51	0.35	0.28	0.22
MgO	2.47	2.31	2.17	1.90
MnO	0.04	0.02	0.02	0.01
P2O5	0.016	0.03	0.01	0.01
SiO2	23.87	17.34	12.60	8.90
TiO2	0.38	0.30	0.24	0.23
Co	< LOD	< LOD	< LOD	< LOD
Pore diameter (nm)	5.19	15.14	7.04	7.04
Pore volume (Cm3/g)	0.003	0.005	0.03	0.03
Surface area (m2/g)	2.59	1.26	0.87	273.58

4.1.4 Brunauer-Emmett-Teller (BET) analysis

The surface area and pore size of the CPNC are the significant properties that influence the sorption of ions by the CPNC. Surface area, pore volume and pore size of nanocomposite was determined using BET method and the results are summarized in Table 5. Table 5 illustrates the distribution of pores of the CPNC, it was observed that the greatest amount of pores lies between 17.34 and 157.22 Å (1.734 nm and 15.722 nm) with the average of pore diameter of 70.457 Å (7.0457 nm). This suggests that the CPNC contains significant amount of small pores ranging from microporous to mesoporous.

Table 5: BET surface area, pore volume and pore width

	CPNCs samples 1	**CPNCs samples 2**	**CPNCs samples 3**	**CPNCs samples 4**
Surface area (m^2/g)				
Single point surface area	2.6471	1.3524	0.9654	101.0585
BET Surface Area	2.5888	1.2568	0.8712	273.5843
BJH Adsorption cumulative surface area of pores	0.468	0.502	0.206	315.302
BJH Desorption cumulative surface area of pores	1.8746	0.7408	2.0937	315.3215
Pore Volume (cm^3/g)				
Single point adsorption total pore volume of pores	0.003360	0.004756	0.002469	0.224882
BJH Adsorption cumulative volume of pores	0.003236	0.006729	0.003336	0.336011
BJH Desorption cumulative volume of pores	0.004481	0.007055	0.003903	0.336418
Pore Size (Å)				
Adsorption average pore width (4V/A by BET)	5.19149	15.13756	11.33657	3.28793
BJH Adsorption average diameter (4V/A)	27.6706	53.5984	64.7922	4.2627
BJH Desorption average diameter (4V/A)	9.5606	38.0923	7.4569	4.2676

4.1.5 Scanning Electron Microscopy (SEM) analysis

Surface topography and composition of Mukondeni black clay was analysed using SEM as seen below in Figure 6a and 6b.

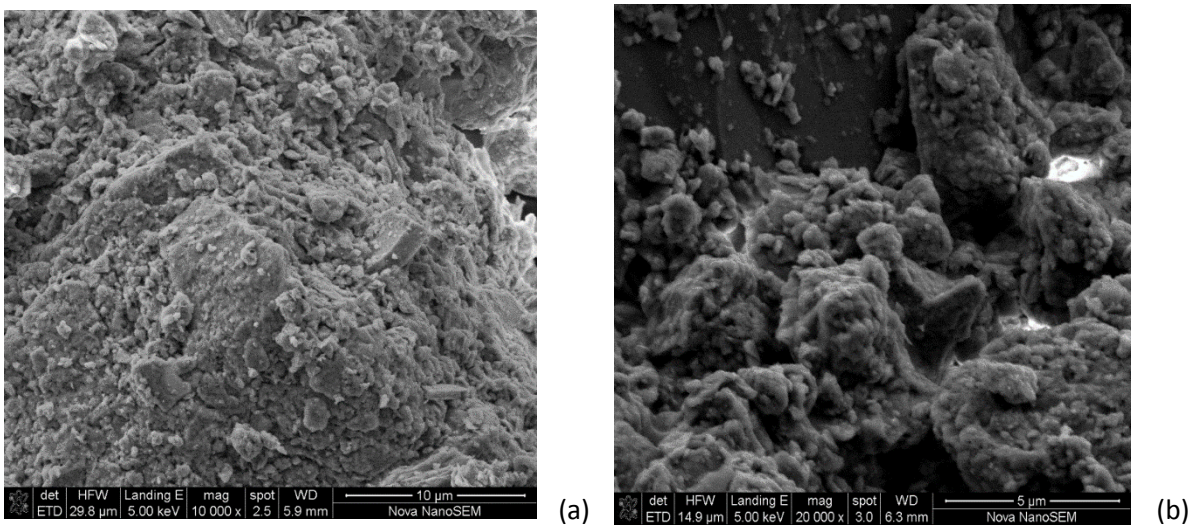

Figure 6a and 6b: Surface morphology of Mukondeni black clay

The surface morphology of Mukondeni black clay at 10 000x and 20 000x magnification is shown in figure 6a and 6b respectively. At lower magnifications, Mukondeni black clay showed irregular rough porous structure and at higher magnifications the image reveals that Mukondeni black clay has a smooth irregular surface. To understand the complex morphologies that occur in the polymer-layered silicate nanocomposites, it is important to review the structural details of layered silicates and their properties. The most heavily used materials in the fabrication of nanocomposites is based on the 2:1 layered structure also known as phyllosilicates, of which the most common representative is montmorillonite (MMT) (Zanetti, et al., 2000). SEM revealed its complex morphological structure.

4.1.6 Fourier Transform Infrared Spectroscopy (FTIR) analysis

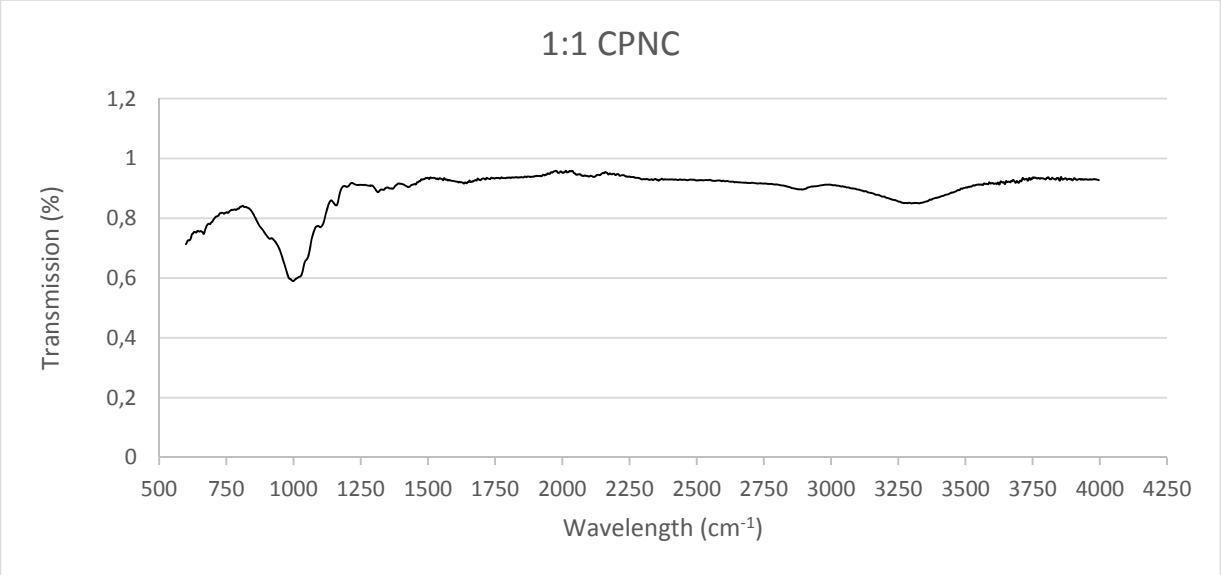

Figure 7a: FTIR spectra of 1:1 CPNC

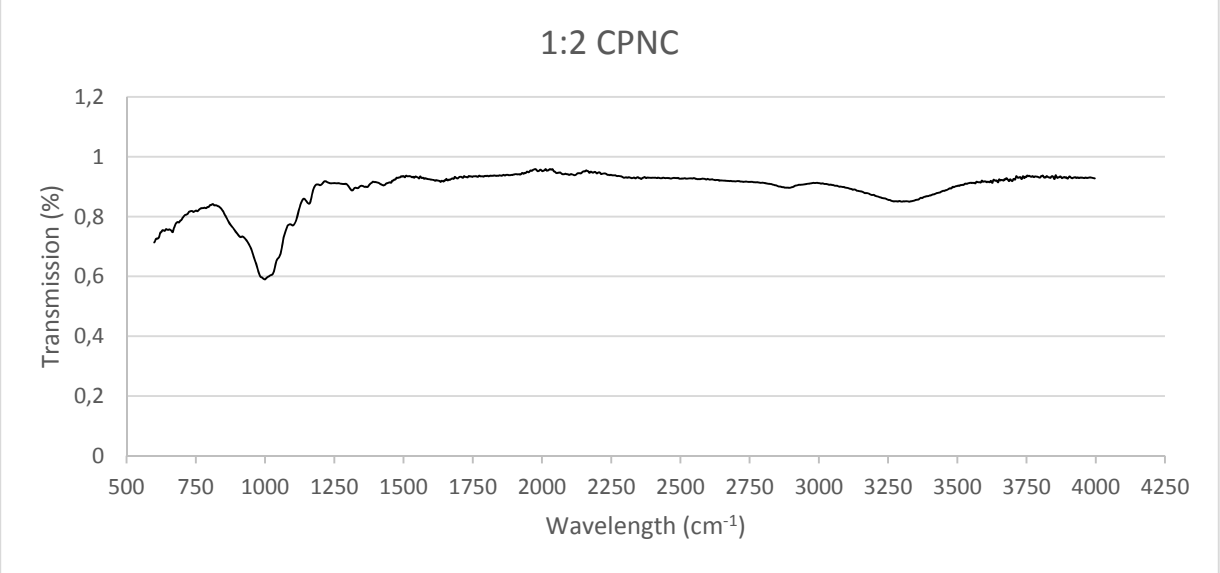

Figure 7b: FTIR spectra of 1:2 CPNC

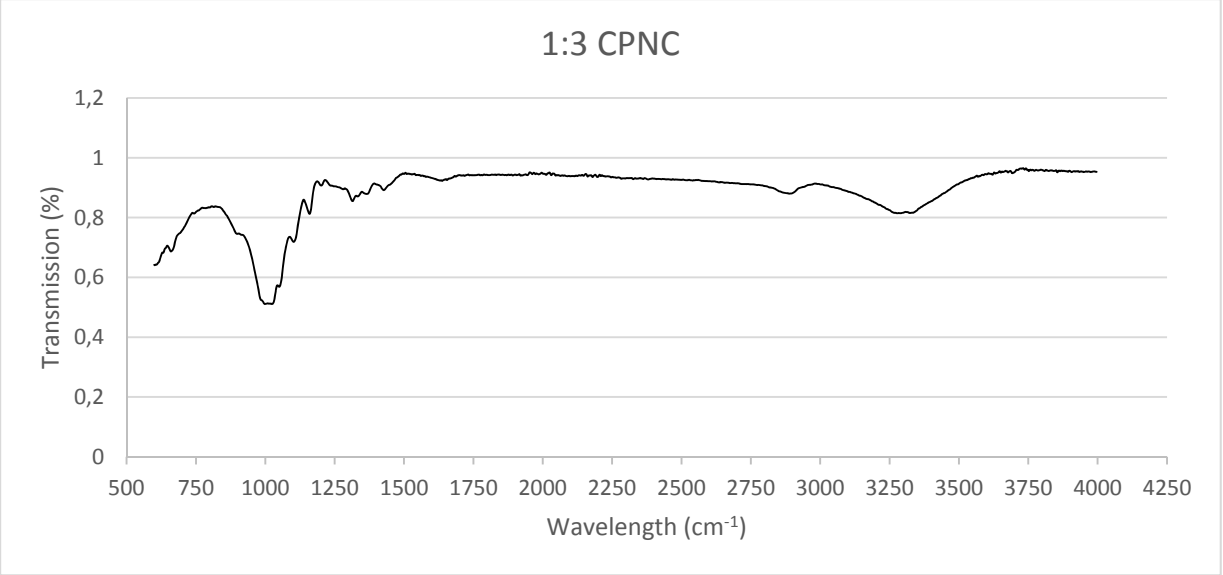

Figure 7c: FTIR spectra of 1:3 CPNC

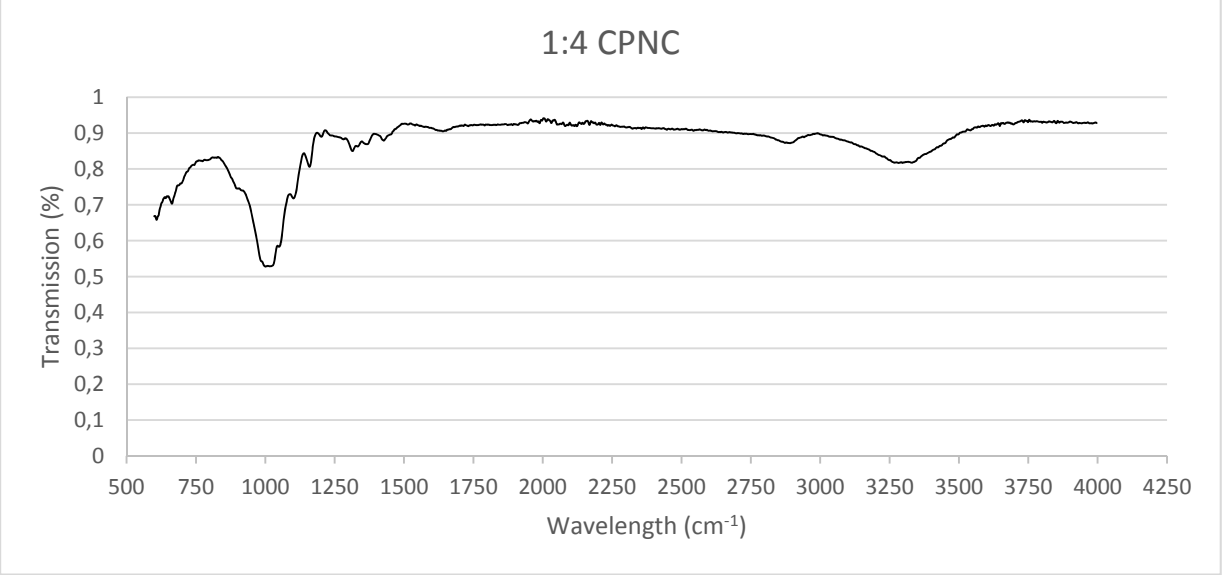

Figure 7d: FTIR spectra of 1:4 CPNC

Figure 7a, 7b, 7c and 7d show the FTIR spectra of CPNC 1:1, CPNC 1:2, CPNC 1:3, and CPNC 1:4 respectively. The most representative bands in all CPNCs can be summarized as follows: The absorption peaks observed at 3348 and 3342 cm^{-1} are due to the stretching vibration of H bonded OH groups of cellulose. This peak shows a lower % transmittance in figure 7a 1:1 CPNC when compared to figure 7d 1:4 CPNC. This higher absorption observed in figure 7d 1:4 CPNC could be due to the presence H_2O contributing to more O-H stretching vibrations. The absorption bands at 2900 and 2970 cm^{-1} correspond to the C-H symmetrical stretching vibration. The C-H bending occurs at 1370 cm^{-1} and 1280 cm^{-1}. The bands at 1432 cm^{-1} and

1316 cm^{-1} in the CPNC spectres are attributed to a symmetric CH_2 bending vibration, in addition, the FTIR absorption peaks between 1027 cm^{-1} and 1058 cm^{-1} represent C-O and C-C stretching bands usually observed in polysaccharides, their increase in transmittance from figure 7a, 7b, 7c and 7d can be attributed to the increase in microcrystal cellulose content in CPNC 1:1, CPNC 1:2, CPNC 1:3, and CPNC 1:4 respectively. The bands between 517 cm^{-1}, 617 cm^{-1}, 669 $cm^{-1}$and 1039 cm^{-1} correspond to the stretching vibrations of Si–O, Al–O, and Mg–O observed for silicate materials.

4.2 Optimisation of fluoride adsorption onto clay polymer nanocomposites

4 samples of CPNC were prepared by varying the ratio of clay to cellulose. Studies on fluoride adsorption using clay have been done before yielding desirable results, in this work, the known properties of clay are combined with cellulose to better improve the properties of the acquired composite which was then synthesised into a CPNC. Varying the clay to cellulose ratio ensured that different ratios were examined, and a more suitable ratio adopted for the adsorption of fluoride from ground water. 4 clay to polymer ratios were prepared via melt intercalation, hence optimization was done to adopt a more suitable ration for the batch adsorption experiments.

In this batch adsorption experiment, 1000 mg/L stock solution of fluoride was prepared by dissolving 2.210g of NaF in 1000 mL of deionized water. The mixture was topped up and thoroughly mixed. From the prepared stock solution, 10 mg/L dilution was made by extracting 10 ml of 1000 mg/L fluoride solution and pipetted into 100 ml volumetric flask. The volumetric flask was topped-up to the mark using deionized water.

All experiment were carried out in triplicate. The samples were filtered through Whatman filter paper No. 42 and the filtrate was analysed for electro conductivity using the CRISON MM40 Multimeter probe and the Orion Versastar fluoride selective electrode for fluoride concentration. TISAB □ was used as buffer for maintaining the ionic strength in the sample during measurement.

4.2.1 Adsorption of fluoride onto clay polymer nanocomposite as a function of contact time

4 samples of 10 ml of 100 mg/L fluoride solution were pipetted into 4 glass beakers and topped up to make a fluoride solution of 10 mg/L in each glass beaker. 1g of different ratios (1:1, 1:2, 1:3 and 1:4) of CPNC was added into each glass beaker. The mixture was then stirred for 1, 5,

10, 15, 30, 60, 120, and 360 minutes using a magnetic stirrer. pH, Temp, and EC was measured by the CRISON multimeter probe (model MM40) before and after stirring. Fluoride was measured by the CRISON multimeter probe.

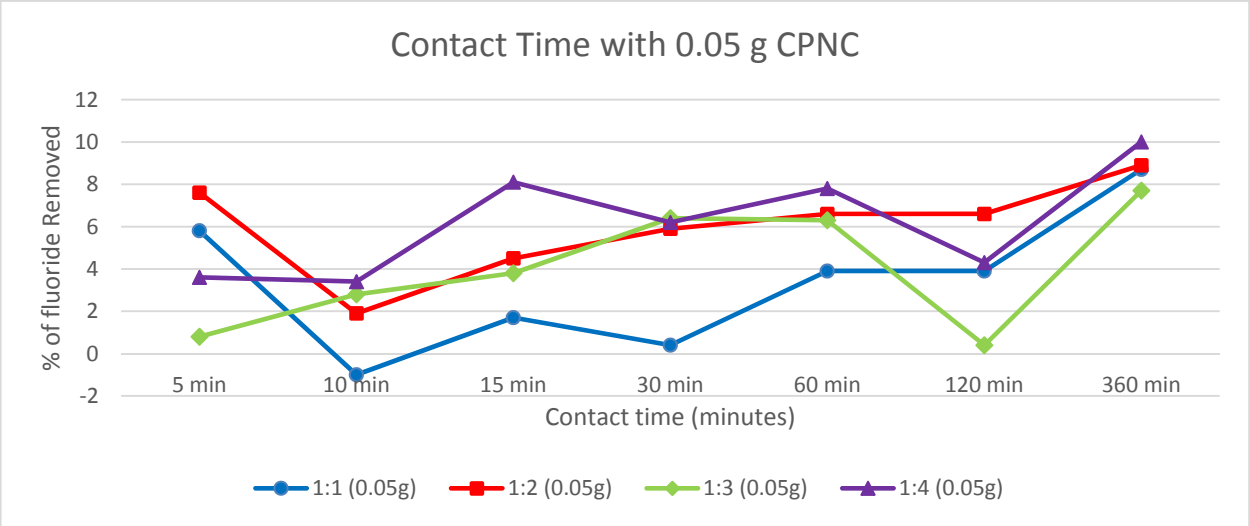

Figure 8a: Variation of different ratios of CPNC % removal for fluoride with contact time (0.05g of adsorbent dosage, 10 mg/L fluoride solution, 7.2 pH, and 26°C)

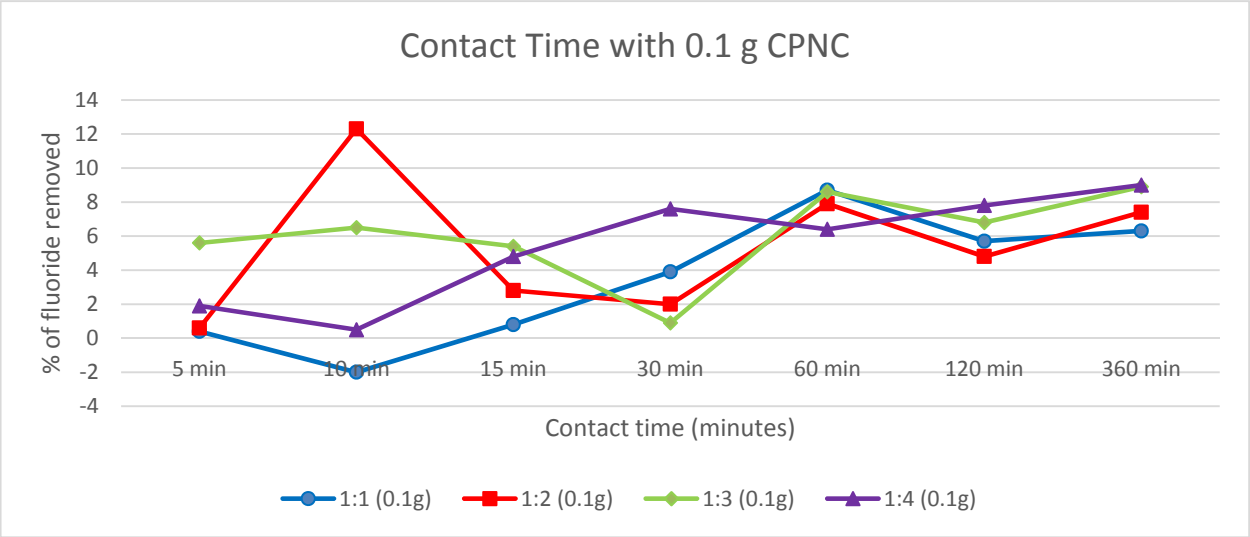

Figure 8b: Variation of different ratios of CPNC % removal for fluoride with contact time (0.1g of adsorbent dosage, 10 mg/L fluoride solution, 7.2 pH, and 26°C)

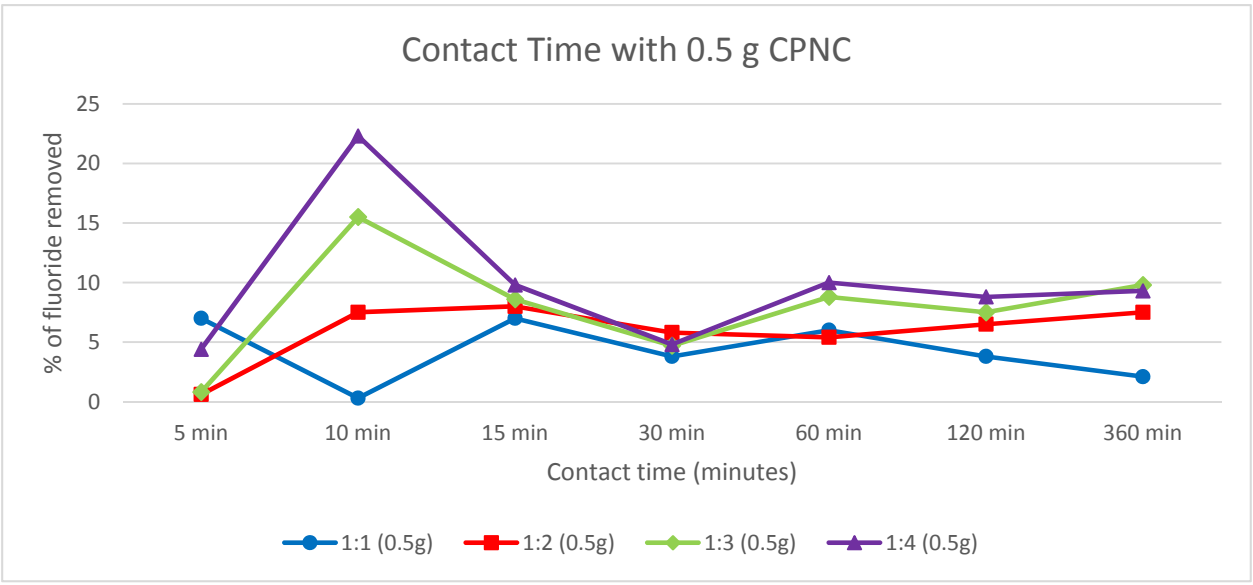

Figure 8c: Variation of different ratios of CPNC % removal for fluoride with contact time (0.5g of adsorbent dosage, 10 mg/L fluoride solution, 7.2 pH, and 26°C)

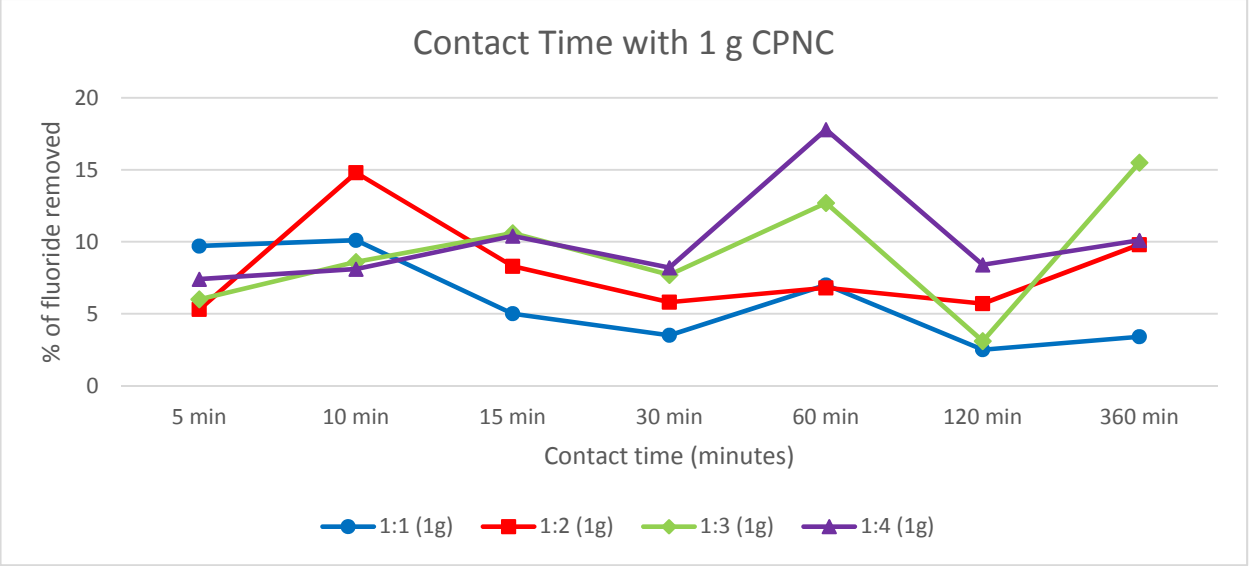

Figure 8d: Variation of different ratios of CPNC % removal for fluoride with contact time (1g of adsorbent dosage, 10 mg/L fluoride solution, 7.2 pH, and 26°C)

Figure 8a shows the sorption of fluoride onto 1:1 and 1:2 CPNCs fluctuating with each time interval. It is clear that in the first 5 minutes of contact time there is a decrease in fluoride absorption while 1:3 and 1:4 CPNC show an increase in fluoride adsorption. Maximum adsorption for fluoride was reached at 360 minutes for all CPNC ratios with an insignificant increase from the initial contact time of 5 minutes. CPNC 1:4 initially removed 3.6% of fluoride after 5 minutes of contact time followed by a slow increase until 360 minutes where in 10% of fluoride was removed. CPNC 1:3 removed an insignificant amount of fluoride initially at a contact time of 5 minutes were in 0.8% of fluoride was removed followed by insignificant fluctuation until a maximum of 7.7% of fluoride was removed at 360 minutes. CPNC 1:2 showed a decrease in adsorption within the first 10 minutes from7.6% removal to 1.9% followed by an insignificant increase to 8.9% at 360 minutes. Similarly, CPNC 1:1 showed a decrease in adsorption within the first 10 minutes from 5.8% to a desorption state of -1% followed by fluctuation until a maximum of 8.7% was removed at 360 minutes.

Figure 8b shows a general increase in adsorption for all ratios as 0.1g of CPNC was used for fluoride adsorption with contact time as a function. A similar trend of adsorption can be observed on 1:4, 1:3, and 1:1 CPNCs of fluctuating adsorption with each time interval. However, maximum adsorption of 12.3% was observed for 1:2 CPNC at 10 minutes. CPNCs 1:4, 1:3 and 1:1 reached maximum adsorption for fluoride at 120, 360 and 60 minutes respectively.

Figure 8c, using 0.5g of CPNC as a function of contact time to remove fluoride, 1:4, 1:3 and 1:2 CPNCs removed more fluoride (22.3%, 15.5% and 7.5% respectively) at 10 minutes as compared to other time interval. However 1:1 CPNC shows desorption at 10 minutes and maximum adsorption of 7% at 15 minutes followed by a decrease in the adsorption capacity until 360 minutes.

Figure 8d shows the adsorption of fluoride using 1g CPNC as a function of contact time onto 1:4 and 1:3 CPNCs increasing with each time interval from the initial 5 minutes were 7.4% and 6% were removed respectively. Both 1:4 and 1:3 follow a similar trajectory of adsorption and desorption pattern reaching maximum adsorption at 60 minutes (17.8% and 12.7% respectively) followed by a decrease at 120 minutes and increase at 360 minutes to 10.1% and 15.5% respectively. It is clear that a general increase in adsorption using 1g as compared to 0.05g in Figure 4a can be observed.

Maximum adsorption of fluoride was attained in 10 minutes using 0.5g of 1:4 CPNC. The preference of fluoride adsorption as a function of contact time using varying ratios of CPNC of different weight was observed to be as follows; 10 minutes using 0.5g of 1:4 CPNC removed 22.3% of fluoride, 60 minutes using 1g of 1:4 CPNC removed 17.8% of fluoride, 10 minutes using 0.5g of 1:3 CPNC removed 15.5% of fluoride, and 360 minutes using 1g of 1:4 CPNC removed 15.5% of fluoride

The low adsorptive characteristic displayed by all 4 CPNCs can be deduced from the BET analysis that revealed low surface area, pore volume, and pore size, it is evident from the BET analysis that less fluoride will be absorb as adsorption sites will be limited.

4.2.2 Adsorption of fluoride onto clay polymer nanocomposites as a function of adsorbent dose

16 samples of 10 ml of 100 mg/L fluoride solution were pipetted into 16 glass beakers and topped up to make a fluoride solution of 10 mg/L in each glass beaker. 4 different masses (0.05 g, 0.1 g, 0.5 g and 1 g) of CPNC were weighed within each ratio (1:1, 1:2, 1:3 and 1:4) of CPNC was added into each glass beaker. The mixture was then stirred for 1, 5, 10, 15, 30, 60, 120, and 360 minutes using a magnetic stirrer. pH, Temp, and EC was measured by the CRISON multimeter probe (model MM40) before and after stirring. Fluoride was measured by the CRISON multimeter probe.

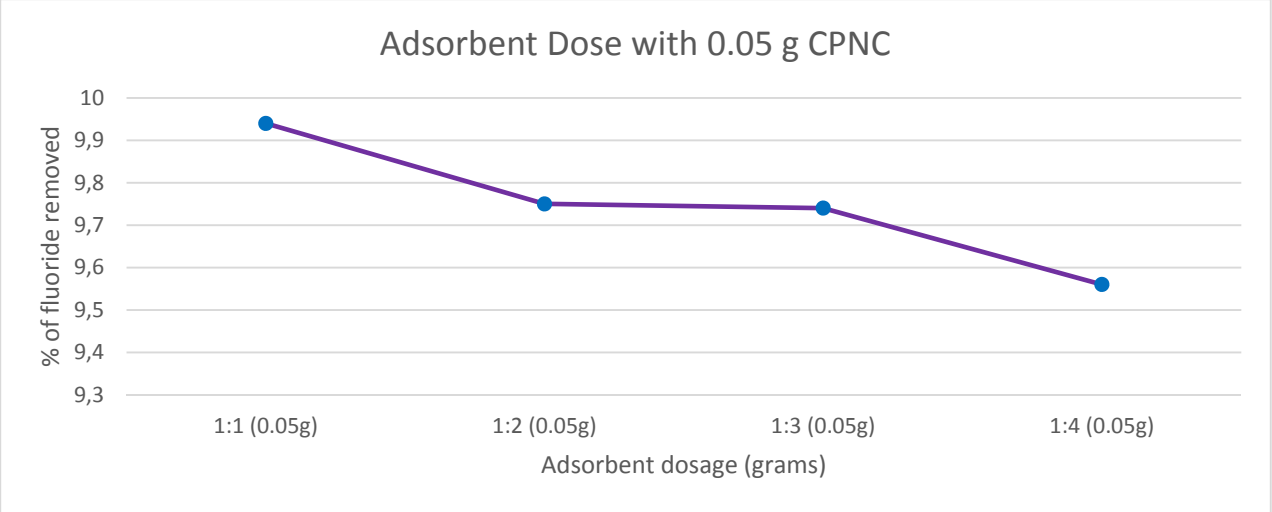

Figure 9a: Variation of adsorption ratio as a function of adsorbent dosage (0.1 g adsorbent, 10 minutes of contact time, 10 mg/L adsorbate concentration, 7 pH, and 26°C)

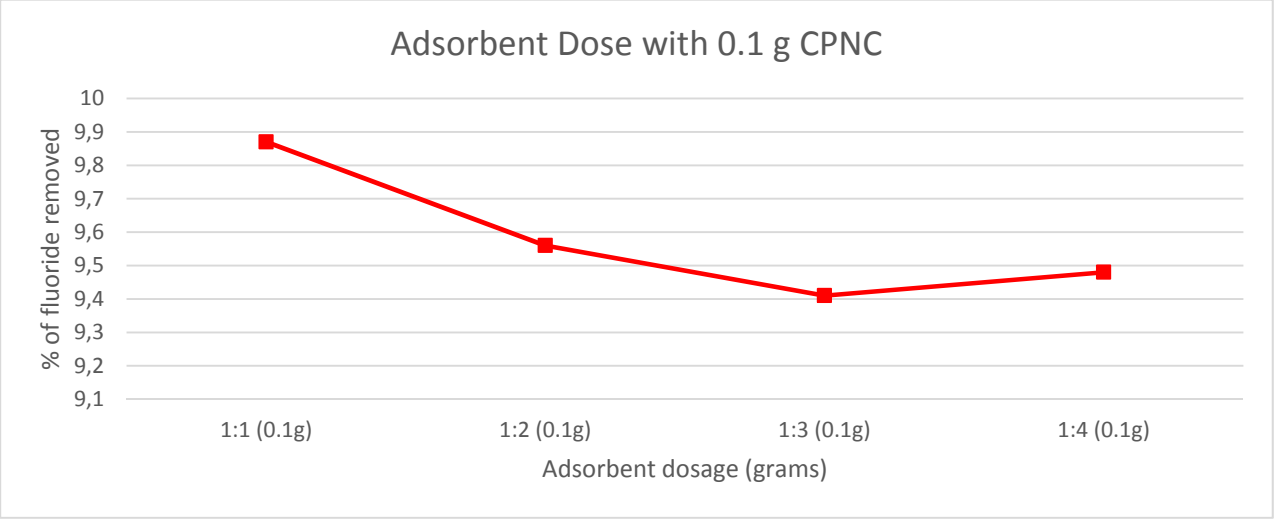

Figure 9b: Variation of adsorption ratio as a function of adsorbent dosage (0.1 g adsorbent, 10 minutes of contact time, 10 mg/L adsorbate concentration, 7 pH, and 26°C)

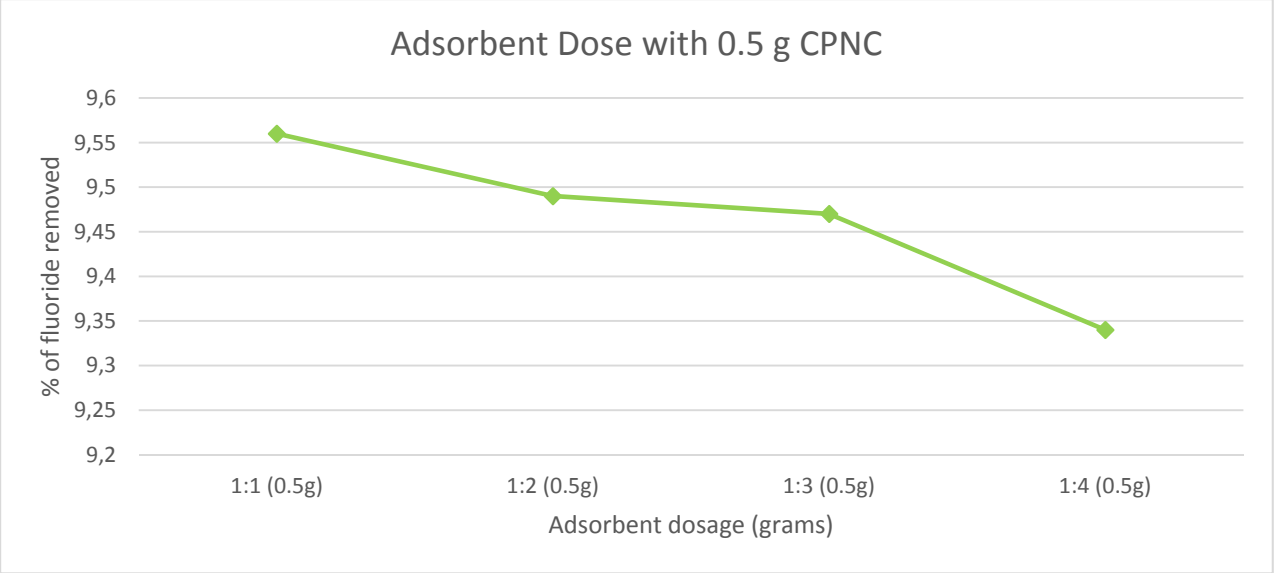

Figure 9c: Variation of adsorption ratio as a function of adsorbent dosage (0.5 g adsorbent, 10 minutes of contact time, 10 mg/L adsorbate concentration, 7 pH, and 26°C)

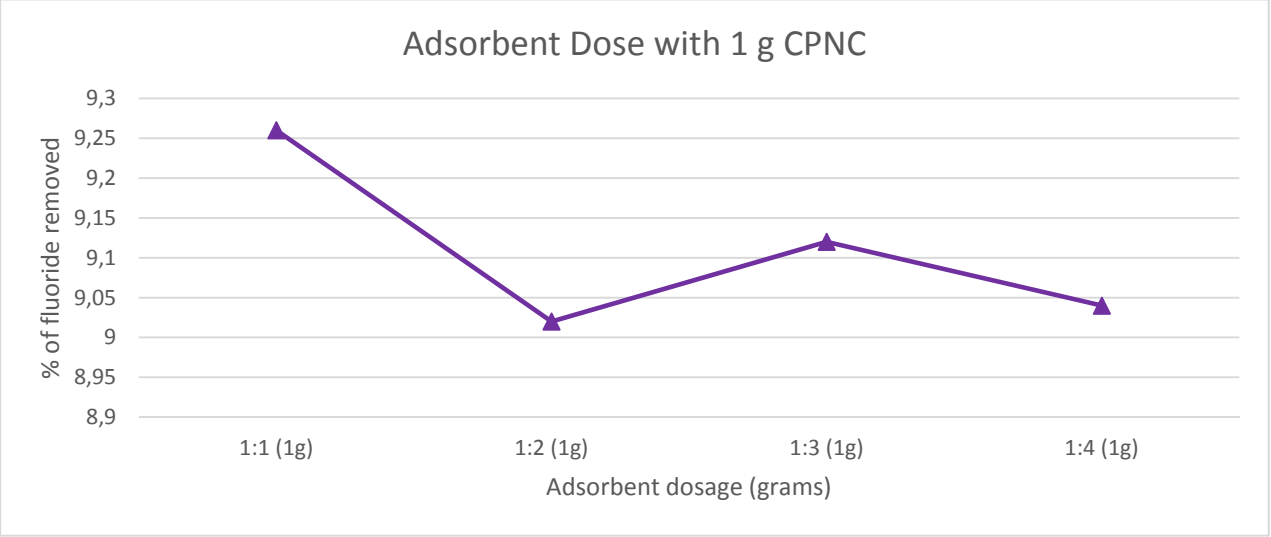

Figure 9d: Variation of adsorption ratio as a function of adsorbent dosage (1 g adsorbent, 10 minutes of contact time, 10 mg/L adsorbate concentration, 7 pH, and 26°C)

The effect of adsorbent dosage was evaluated by varying the amount of CPNC from 0.05 g/100 mL to 1 g/100 mL .An initial fluoride concentration of 10 mg/L was used. Figure 9a, 9b, 9c and 9d shows the results reported as percentage of fluoride removal. Adsorption of fluoride was observed to increase with adsorbent dosage for all 4 ratios of CPNC. It can be observed that fluoride removal increased gradually from 9.04% at an adsorbent dosage of 0.05 g of 1:1

CPNC to 9.94% at an adsorbent dosage of 1g of 1:4 CPNC. The insignificant increase is likely a result of an enhancement in the number of adsorption active sites available for adsorption of F^- as the adsorbent mass increased. An overall slight insignificant change in the percentage of fluoride removal can be observed for an adsorbent dosage of 0.05g, 0.1g and 0.5g which may be an indication that the CPNCs have reached equilibrium. Similar results have been reported by Kamble et al. 2010, with chemically modified bentonite for which they cited two reasons: (1) better utilization of the available active sites at low adsorbent dose in comparison to high adsorbent dose at which too many sites are available for limited quantity of adsorbate and (2) reduced driving force for adsorption as high adsorbent dose causes lower equilibrium fluoride concentration.

4.2.3 Adsorption of fluoride onto clay polymer nanocomposites as a function of pH

20 samples of 10 ml of 100 mg/L fluoride solution were pipetted into 20 glass beakers and topped up to make a fluoride solution of 10 mg/L in each glass beaker. The pH was adjusted using 0.1 M HCL and 0.1 M NaOH to 2, 5, 7, 9 and 12. 0.05 g, 0.1 g, 0.5 g and 1 g of CPNC of different ratios (1:1, 1:2, 1:3 and 1:4) was added into each glass beaker. The mixture was then stirred for 30 minutes using a magnetic stirrer. pH, Temp, and EC was measured by the CRISON multimeter probe (model MM40) before and after stirring. Fluoride was measured by the CRISON multimeter probe.

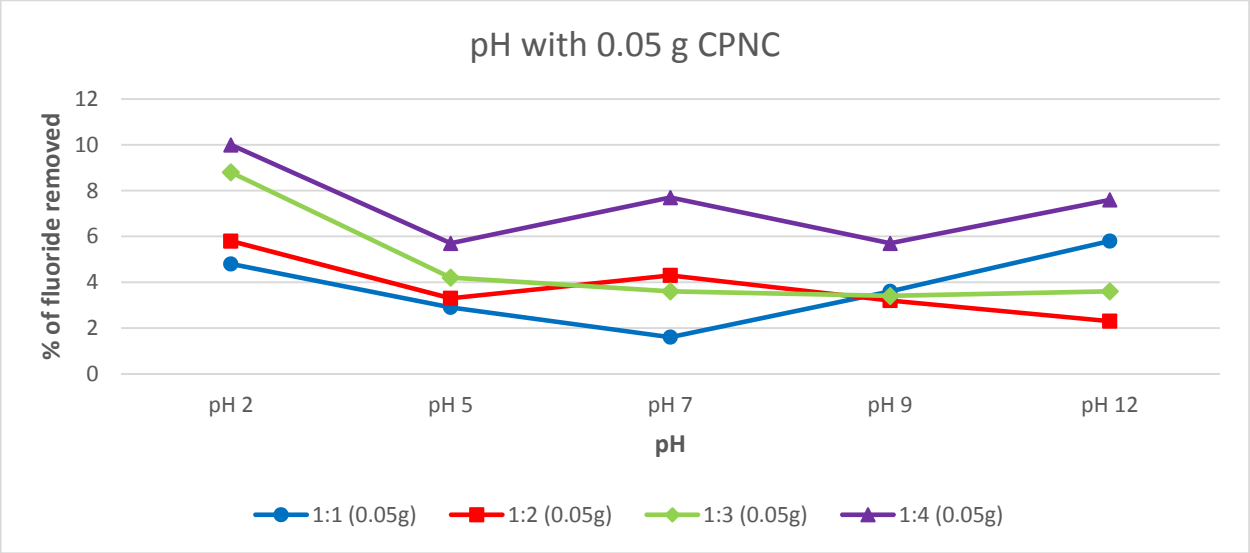

Figure 10a: Variation of adsorption ratio with varying pH (0.05 g adsorbent, 10 minutes of contact time, 10 mg/L adsorbate concentration, and 26°C)

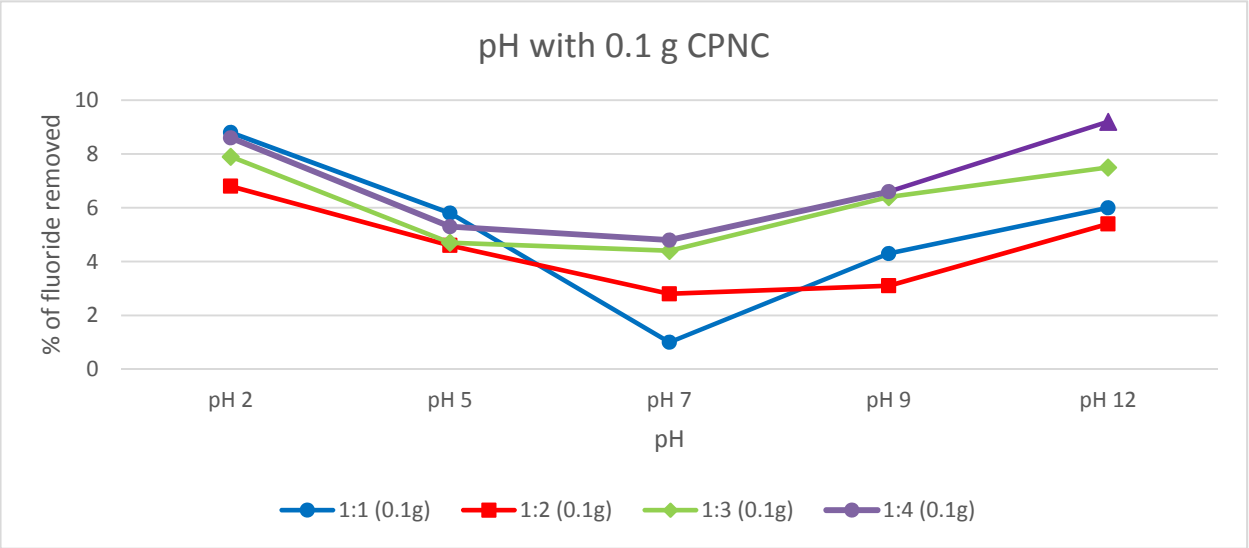

Figure 10b: Variation of adsorption ratio with varying pH (1 g adsorbent, 10 minutes of contact time, 10 mg/L adsorbate concentration, and 26°C)

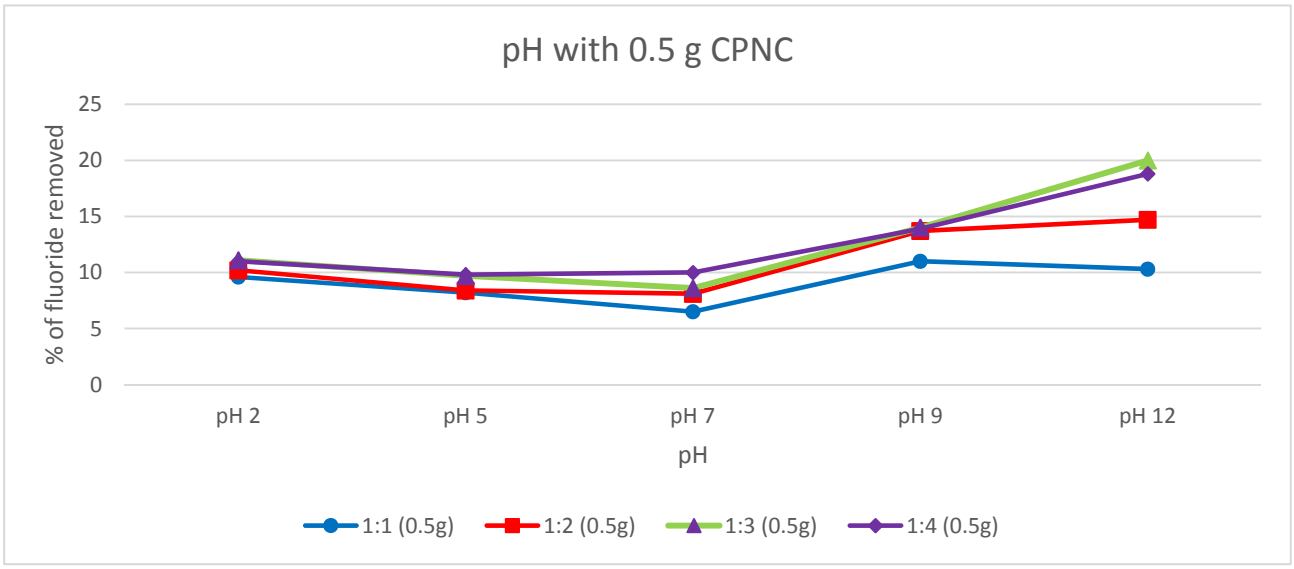

Figure 10c: Variation of adsorption ratio with varying pH (0.5 g adsorbent, 10 minutes of time, 10 mg/L adsorbate concentration, and 26°C)

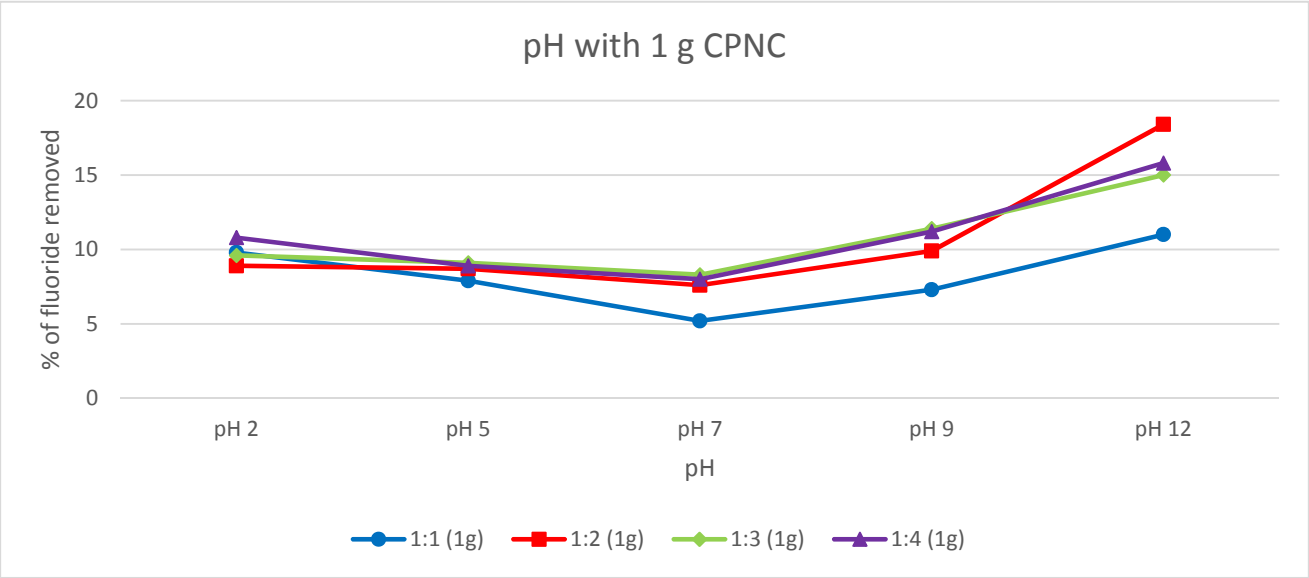

Figure 10d: Variation of adsorption ratio with varying pH (1 g adsorbent, 10 minutes of contact time, 10 mg/L adsorbate concentration, and 26°C)

Figure 10a, 10b, 10c and 10d presents the results of fluoride removal when varying the pH of the solution from 2 to 12 using 0.1 M NaOH and 0.1 M HCl. pH of the medium is one of the important parameters that influence fluoride removal efficiency significantly and help to understand the fluoride-uptake mechanism of the adsorbent. From the results presented in Figure 10d, it is evident that CPNC showed fluoride removal efficiency in the range of 2 and 12 pH. The optimal pH – with a fluoride removal of about 18.8% – was basic with a pH of 12. A minimum decrease in adsorption was observed at pH 7 in Figure 10a at 1% fluoride removal. At pH 2 the surface of the clay is positively charged and F- would be electrostatically attracted to the clay surface, which explains the high F- adsorption at pH 2. The trend of change in pH during fluoride adsorption showed that at a pH between 5 and 9, there was a decrease in fluoride adsorption as compared to higher (above 9) pH values. The increase may be attributed to the release of OH- ions from the adsorbent surface during ion exchange and the decrease in final pH at initial pH above 9 may be attributed to the release of H+ ions from the adsorbent surface.

The adsorption of fluoride onto CPNC was highest at 17.8% at 60 minutes (1:4 CPNC), 22.3% for all pH conditions. The results indicate that acidic and basic pH are the regions where optimum removal of fluoride occurred.

4.2.4 Adsorption of fluoride onto clay polymer nanocomposites as a function of adsorbate dose

To evaluate the effect of adsorbate dose 16 samples of 4 5 mg/L fluoride solution, 4 10 mg/L fluoride solution, 4 20 mg/L fluoride solution and 4 50 mg/L fluoride solution. 1 g of CPNC 1:1, 1:2, 1:3 and 1:4 were added into the varied adsorbate dose sample in polyethylene plastic bottles. The pH was adjusted using 0.1 M HCL and 0.1 M NaOH to 2, 5, 7, 9 and 12. 0.05 g, 0.1 g, 0.5 g and 1 g of CPNC of different ratios (1:1, 1:2, 1:3 and 1:4) was added into each glass beaker. The mixture was then stirred for 30 minutes using a magnetic stirrer. pH, Temperature, and EC was measured by the CRISON multimeter probe (model MM40) before and after stirring. Fluoride was measured by the CRISON multimeter probe.

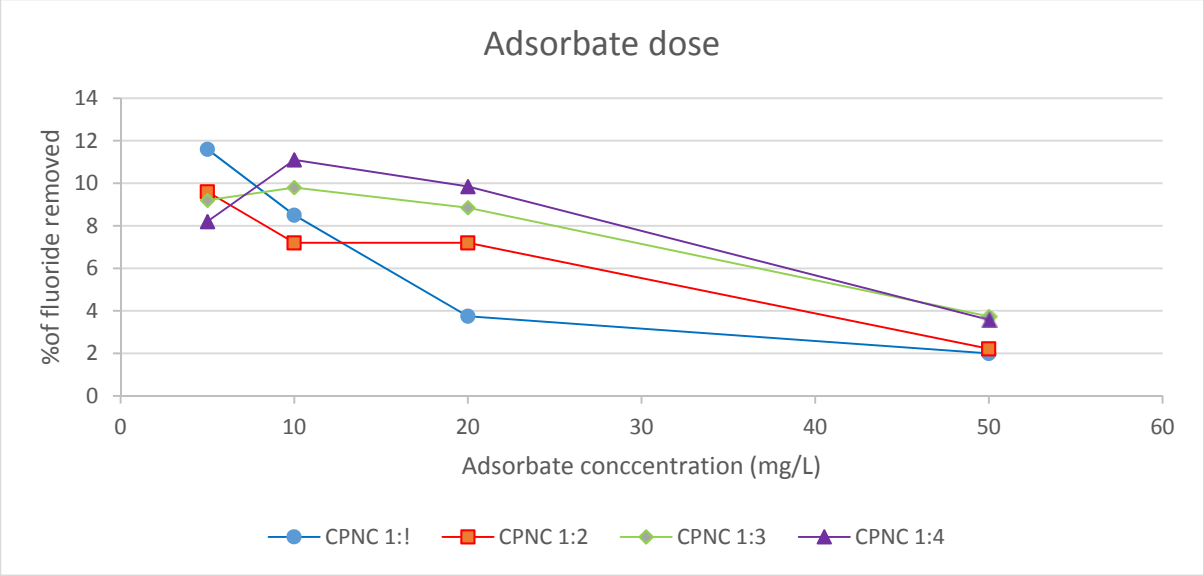

Figure 11: Variation of adsorption ratio with varying adsorbate concentration (1 g adsorbent, 10 minutes of contact time, and 26°C at 250 rpm shaking speed)

It can be observed that the % F^- removal decreases with increased fluoride concentration. The decrease in fluoride adsorption can be attributed to the availability and increase of fluoride ions in solution at high fluoride concentration, this further indicates that the CPNCs get exhausted as adsorption sites reach equilibrium.

4.2.4 Optimisation conclusion

Polymer nanocomposites are known for highly tuneable adsorption behaviour due to the presence of nano particles with high surface area in the polymer matrix. Optimized adsorption behaviour of nanocomposites make them suitable for different technical applications; and in

this study fluoride adsorption. However, CPNCs synthesized in this study are not efficient fluoride adsorbent as they could not remove 50% of fluoride in solution as batch optimization was conducted. Though the basic objective was to improve the compatibility, ion exchange and surface interaction to efficiently adsorb fluoride from solution, CPNCs prepared via melt intercalation with different ratios of Mukondeni black clay to microcrystalline cellulose and glycogen used a binder removed 23% of fluoride at most. Fluoride adsorption depends on ionic or surface interaction, which needs selective interaction site. The prepared CPNCs are not appropriate substrates for this purpose, this may be due to traces of the incinerated poly ethylene glycol acting as a binder in the mixture between cellulose and clay before melt-mixing. The designing of correct preparation techniques is very critical to obtain nanocomposites with desirable properties. Polymer melting points and evaporation point of the binder should be taken into consideration. Poly ethylene glycol have been reported as low-melting solids depending on their molecular weights. The presents of small trace amount of poly ethylene glycol might decrease the fluoride adsorptive ability of the CPNC though CPNCs have high surface area and are used in water purification (Daer, 2015). The structure of poly ethylene glycol $H\text{-}(O{-}CH_2{-}CH_2)_n{-}OH$ has been reported to release –OH hence the higher adsorptive ability of the CPNCs at acidic conditions as compared to alkaline basic condition. Highly alkaline basic condition have been reported to favor the formation of agglomerates which restricts maximum adsorptive abilities of an absorbent and its use.

The surface area and pore size of the CPNC are significant properties that influence the sorption of ions by the CPNC. Surface area, pore volume and pore size of nanocomposite determined using BET showed less surface area as compare to modified smectite clay. This may be due to the degree of compatibility between polymer and modified clay. Another important strategy to optimize adsorption behaviour is to synchronize hydrophobic and hydrophilic behaviour in composite matrix thereby matching the affinity of the polymer and clay. Different polymers have different affinity to clay and this is influential to the CPNC's adsorptive ability.

FTIR analysis should be carried out to supplement and add more details on the mineralogical and chemical properties of the CPNCs as limit of detection occurred on other elements within the CPNCs, during XRF analysis, this will further shed light on whether poly ethylene glycol was completely incinerated before the composites where inserted into the extrude.

However, in the course of adsorption many secondary elements may also be generated there by competing for active adsorption site with F^- further limiting the adsorptive ability of the CPNCs.

4.3 Regeneration adsorption of clay polymer nanocomposites

The regeneration potential of CPNCs was evaluated through 3 successive adsorption desorption cycles performed at an initial concentration of 10 mg/L F^-, contact time 10 minutes at pH 7.2, figure 11 presents the results.

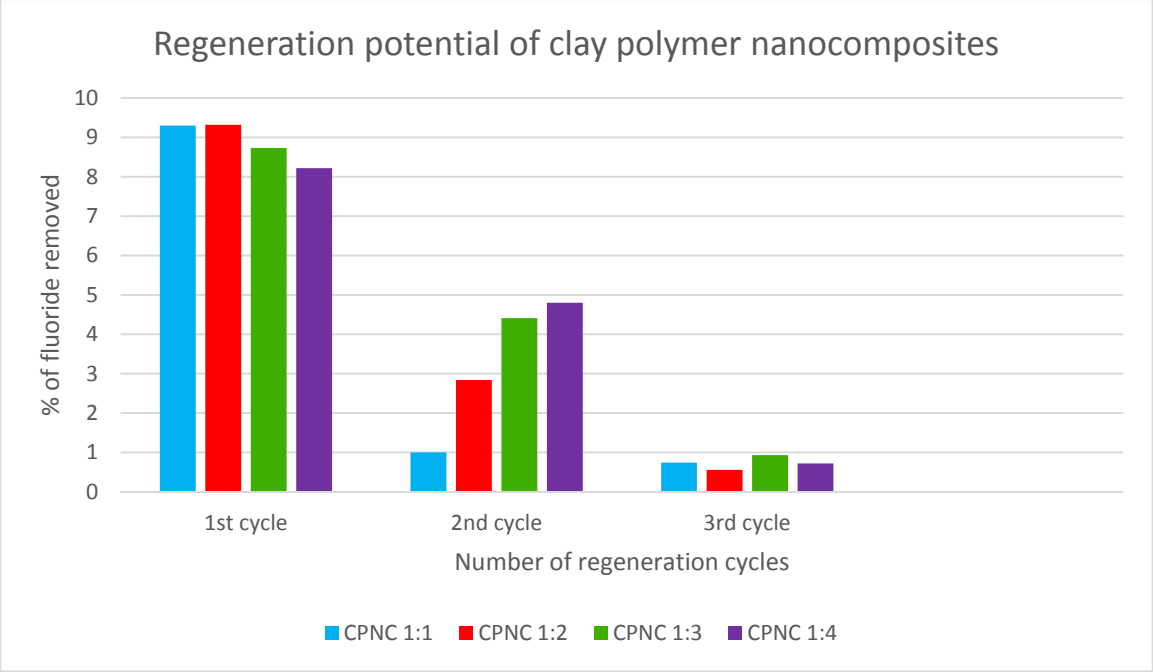

Figure 12: Regeneration of clay polymer nanocomposites (10 mg/L, 10 minutes contact time, pH 7.2 at 250 rpm).

It is clear from that results that percentage of fluoride removal decreased after the first cycle for all ratios of CPNCs, a continued decreased can be observed following the second cycle. CPNC 1:2 decreased from 9.32 % at the 1st cycle to 2.84 % and 0.56 % on the 2nd and 3rd cycle respectively. CPNC 1:4 decreased from 8.22 % at the 1st cycle to 4.80 % and 0.72 % on the 2nd and 3rd cycle respectively. The decreased in adsorptive capacity is more likely due to inadequate regeneration of the adsorbent as similar trends have been report in literature, *Jia, et al., (2005)* and *Zhang, et al., (2011)*.

4.4 Defluoridation of field water

Clay polymer nanocomposites were tested for fluoride removal using field groundwater collected from Siloam borehole, Nzhelele in Limpopo province. The initial fluoride

concentration for the collected field groundwater was 5.4 mg/L, EC 436 µS/cm, and TDS 282 mg/L.

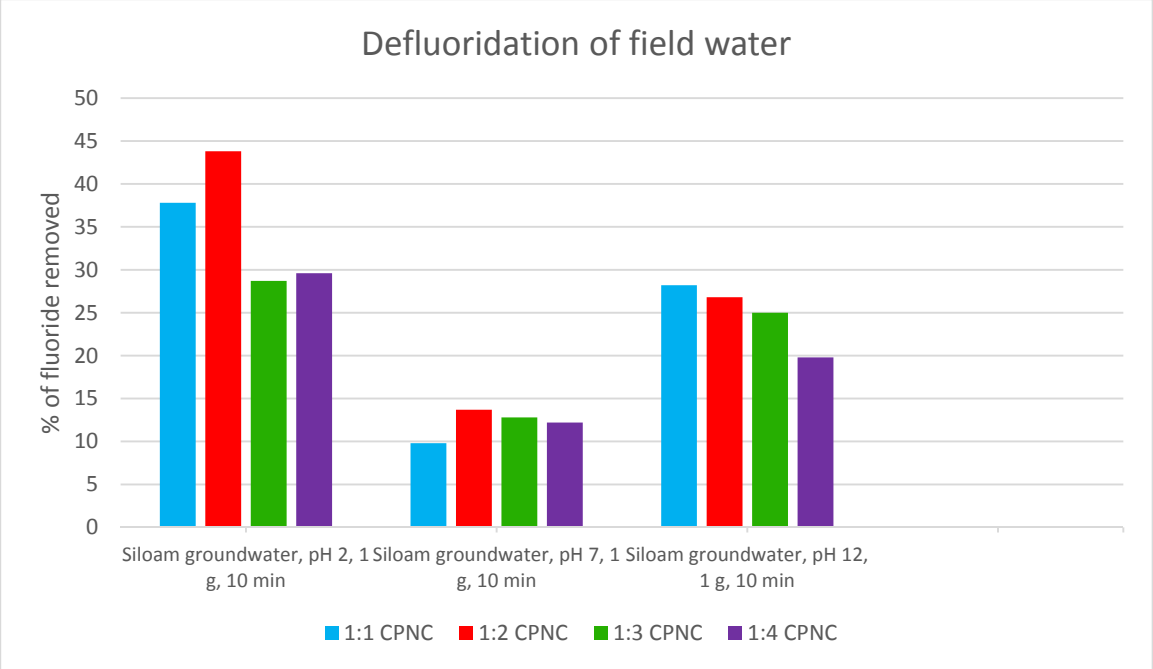

Figure 13: Defluoridation of field water

Figure 12 shows the removal efficiency of fluoride from field groundwater (Siloam groundwater) using CPNCs. The fluoride-rich Siloam groundwater had a slightly alkaline pH of 9.6. CPNC 1:1 removed 37 % of fluoride at pH 2, 9.8 % at pH 7 and 28.2 % at pH 12. CPNC 1:2 removed the most fluoride (43.8 %) at pH 2 and had a significant decrease in adsorption at pH 7 and further removed 26.8 % at pH 12. CPNC 1:3 and 1:4 removed 28.7 % and 29.6 % of fluoride from Siloam groundwater at pH 2, 12.8 % and 12.2 % at pH 7 respectively and further removing 25 % and 19.8%.

The significant rise in adsorption of CPNCs at pH 2 may be attributed to the H 3O Þ ion making the CPNC surface positively charged and hence was accessible for fluoride ions. The decrease in fluoride adsorption at pH 7can be attributed to the competition of active sites on CPNCs surface between OH^- and F^-. Carbonate is one of the greatest competitors for fluoride adsorption followed by phosphate and sulphate, their presents in groundwater may decrease the adsorption of fluoride as seen in the figure above at pH 7.

4.5 Adsorption kinetics

Adsorption kinetics are useful for the prediction of adsorption rate that gives important information for modelling the process and designing CPNCs (Yousef et al., 2011). In this work Pseudo-first order and Pseudo-second order kinetic models were used to analyse the fluoride adsorption kinetics data. The applicability of these models for the fluoride adsorbent on CPNCs was evaluated for the goodness of data fit, coefficient of determination (R^2), and comparison of experimental and predicted amounts of fluoride adsorbed at equilibrium qe (mg/g).

The mathematical representation of the first and second-order kinetic models are given in equations (4) and (5) respectively, which can be integrated to obtain the respective linear forms given by figure 13 and 14.

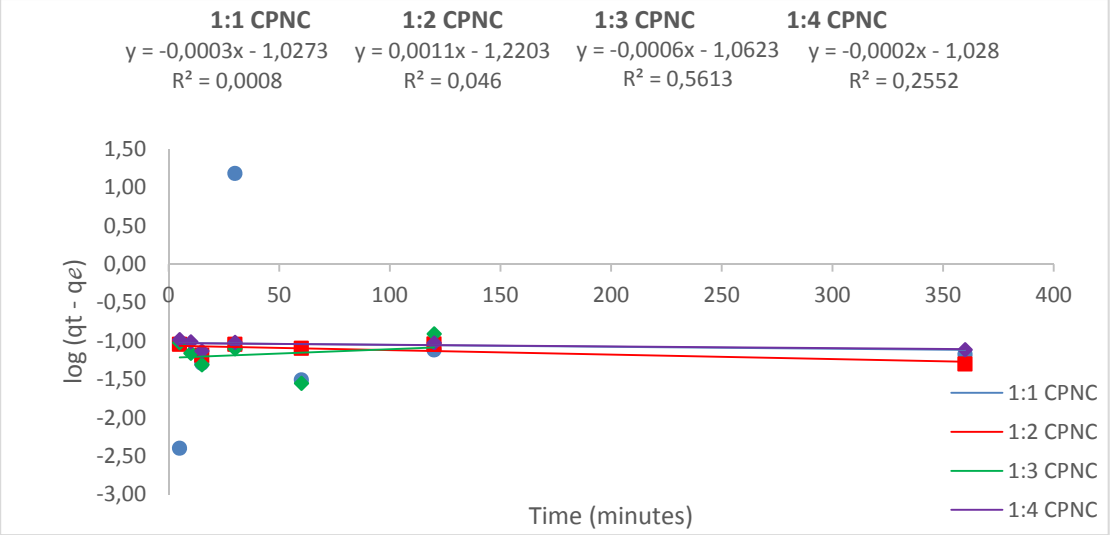

Figure 14: Pseudo first order plot at various adsorbent dose (10 mg/L F^-, pH 7.2 and 250 rpm shaking)

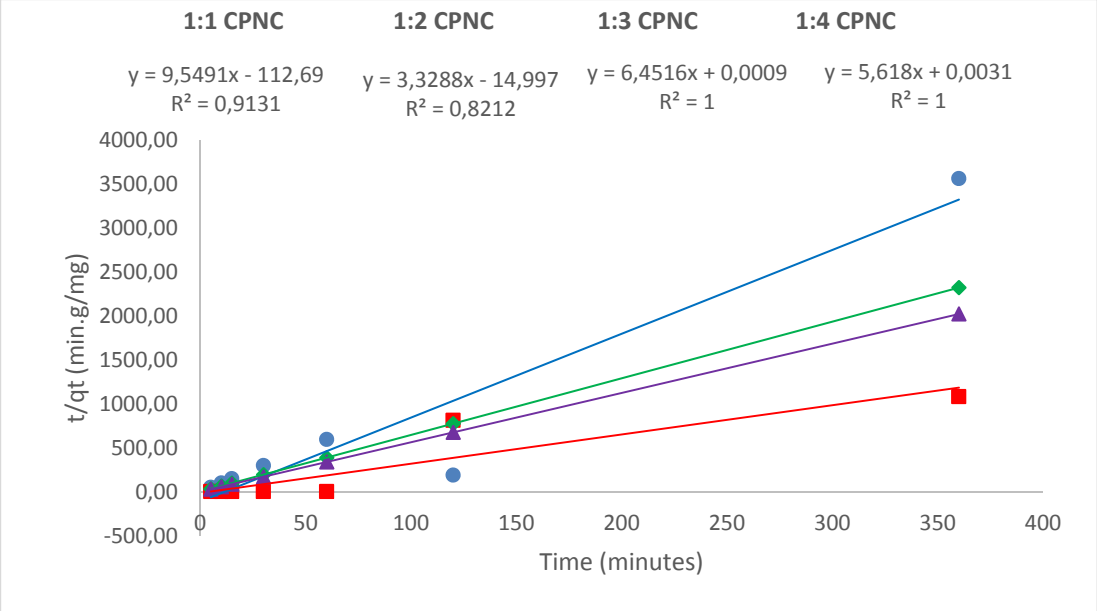

Figure 15: Pseudo second order plot at various adsorbent dose (10 mg/L F^-, pH 7.2 and 250 rpm shaking)

The adsorption kinetics data for CPNCs fitted better with the pseudo second order kinetic model based on the R^2 values. The pseudo first order kinetic model predicted significantly lower values of equilibrium adsorption capacity (qe) than the experimental values qe (exp.), which suggests that the adsorption process of fluoride onto CPNCs is not a first order reaction. On the other hand the theoretical (qe.) values determined from the second order model were in good agreement with the experimental values qe (exp.) (Table 6), which further shows the applicability of the model to describe the adsorption process of fluoride on CPNCs. The model is based on the assumption that the fluoride adsorption process follows a second order chemisorption.

Table 6: Kinetic parameters for fluoride adsorption by CPNCs

	Pseudo first order			Pseudo second order		
	q□ (mg/g)	K*ad* (min^{-1})	R^2	K_{2ad} ($g.mg^{-1}$ min^{-1})	q□ (mg/g)	R^2
CPNC 1:1	0.101	-1292	0.0008	49.50	0.097	0.9131
CPNC 1:2	0.083	-1.187	0.046	67.57	0.146	0.8212
CPNC 1:3	0.086	-1.161	0.5613	96.77	0.106	1
CPNC 1:4	0.178	-1.027	0.2552	337.08	0.178	1

4.6 Adsorption modelling

The basic assumption in deriving the Langmuir model is that adsorption occurs at specific homogenous sites within the adsorbent by monolayer sorption, without interaction between adsorbate molecules. It further assumes that once an adsorbate occupies a particular site, no further adsorption can occur at that site. Thus in theory, a saturation point is reached where all active sites are occupied, and no further adsorption can occur.

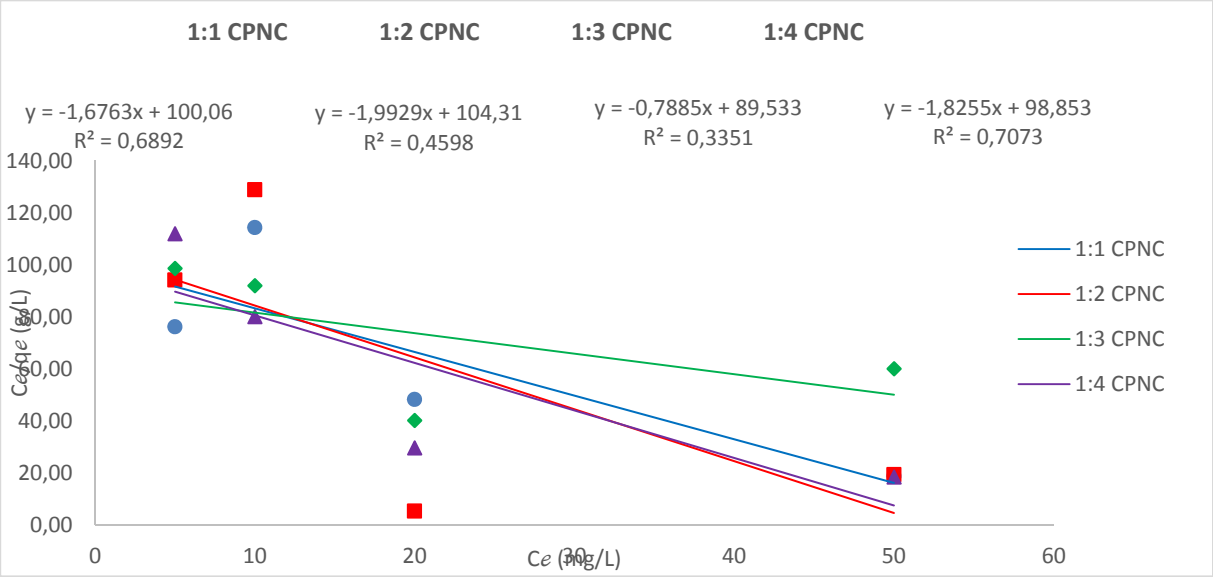

Figure 16: Langmuir isotherm (contact time 30 min, adsorbent dose 0.1 g/100 mL at 250 rpm shaking speed)

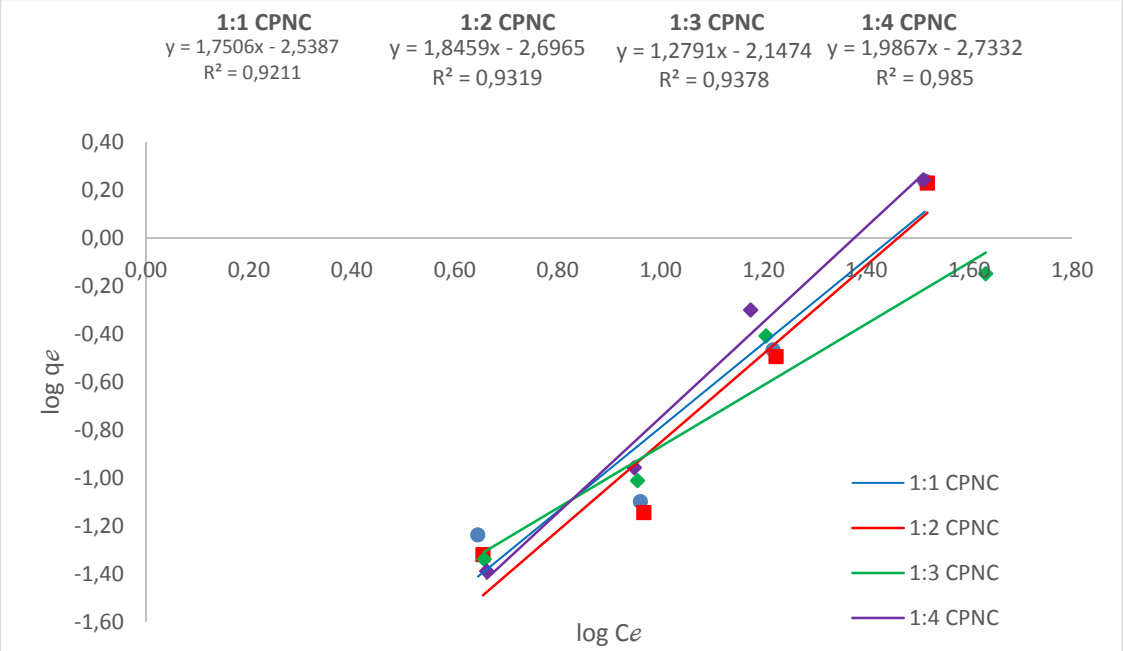

Figure 17: Freundlich isotherm (contact time 30 min, adsorbent dose 0.1 g/100 mL at 250 rpm shaking speed)

The Langmuir and Freundlich isotherm plots of the equilibrium data for fluoride uptake by CPNCs are shown in Figure 15 and 16 respectively. The isotherm constants, calculated from the slopes and intercepts of the linear plots of the equilibrium data according to Langmuir and Freundlich equations, respectively, are presented in Table 7. The high R^2 values indicate that Freundlich model was the best fit for the data able to reasonably describe the equilibrium uptake of fluoride onto CPNCs. The applicability of Frendlich model suggests that there are heterogeneous active binding sites on the surfaces of CPNCs. These binding sites would be involved in multilayer adsorption of the fluoride ions and the adsorption mechanism may involve physical adsorption processes (Bansal and Goyal, 2005; Hayes and Mabaga, 2013; Aziz and Mojin, 2014).

Table 7: Langmuir and Freundlich isotherm models (contact time 30 min, adsorbent dose 0.1 g/100 mL, 250 rpm shaking speed)

	Langmuir isotherm			Freundlich isotherm		
	qm (mg/g)	b (L/mg)	R^2	K_t (mg/g)	1/n	R^2
CPNC 1:1	0.058	0.652	0.6892	0.58	0.645	0.9211
CPNC 1:2	0.048	0.566	0.4598	0.048	0.655	0.9319
CPNC 1:3	0.089	0.632	0.3351	0.046	0.657	0.9378
CPNC 1:4		0.698	0.7073	0.041	0.662	0.985

CHAPTER FIVE

Conclusions and Recommendations

5.1 Conclusions

This study was designed in an attempt to answer the following questions governed by the objectives regarding the synthesis, characterization and performance evaluation of groundwater defluoridation capacity of clay polymer nanocomposites.

- How to modify clay layers?
- What are the physicochemical properties of clay polymer nanocomposites?
- What are the optimum conditions for F^- removal using clay polymer nanocomposites?
- What is the regeneration potential of clay polymer nanocomposites?

The following discussion will attempt to evaluate and elucidate more on the success and drawbacks of the study with regard to each of the above questions and will also give recommendation on the synthesis and use of CPNC and future work emphasis.

5.1.1 Modification of clay layers

This clay modification method was found to have been adopted from *Singla, et al, 2012*, Clay modification by the use of organic cations.

Natural Mukondeni black clay was successfully modified by ion exchange adding 60 g in 600 mL ultra-pure water containing 2.5M HCL, stirring the solution at 360 rpm for 3 hours at 60 ○C using a magnetic stirrer. The obtained clay sample was modified with, ammonium hydroxide and further dissolved in 500 mL of distilled water before filtration and washing with distilled water repeated than dried. XRD spectra revealed that the clay was mainly characterized of Quartz, Albatite, Montmorillonite, Ednite and Magnesium. XRF results further confirms smectite (60.34 %) as the major mineral and quartz (20.21 %) and plagioclase (20.39 %) as minor minerals constituting the modified Mukondeni black clay.

5.1.2 Physicochemical and mineralogical characterisation of clay polymer nanocomposites

Mineralogical composition of the clay polymer nanocomposite was evaluated using XRD, elemental composition was evaluated using XRF, surface morphology using SEM, surface area using BET, functional groups using FTIR, and CEC using ammonium acetate method. The

following conclusions were drawn on the physicochemical and mineralogical properties of the CPNC.

CPNC 1:1 revealed cellulose, Quartz and Albatite as the major minerals with traces of Montmorillonite, Ednite and Magnesium as minor minerals constituting the CPNC 1:1. A change from an amorphous phase to a partly amorphous-partly crystalline phase was observed as CPNC 1:2, 1:3 and 1:4 assumed less Mukondeni clay content and more cellulose content.

It was observed through XRF that silica (SiO_2) was not the main component of the CPNC 1:2, CPNC 1:3 and CPNC 1:4 as it averaged 23.87% followed by Al_2O_3 with an average of 5.34%, the make-up bulk material was cellulose ($C_6H_{10}O_5$). High concentration of SiO_2 and Al_2O_3 reveal that the CPNC is partially an alumino-silicate material.

BET revealed that the greatest amount of pores in CPNCs lies between 17.34 and 157.22 Å (1.734 nm and 15.722 nm) with the average of pore diameter of 70.457 Å (7.0457 nm) suggesting that the CPNC contains significant amount of small pores ranging from microporous to mesoporous.

5.1.3 Adsorption capacity and regeneration of clay polymer nanocomposites

Fluoride adsorption as a function of contact time using varying ratios of CPNC of different weight was observed to be 0.5g of 1:4 CPNC removed 22.3% of fluoride at 10 minutes. The results also indicate that acidic and basic pH are the regions where optimum removal of fluoride occurred.

Fluoride adsorption of groundwater onto CPNCs of high fluoride borehole water from Siloam with an initial concentrations of 6.45 mg/L revealed through a series of batch adsorption experiments that 43.8 % F^- removal at initial concentration of 10 mg/L F^-, pH 2, 1 g CPNC with 10 minutes contact time was achieved. The CPNC exhibited 43.8 % and 28.2 % F^- removal at a pH of 2 and 12 respectively. CPNC showed <50% efficiency for fluoride removal.

Adsorption kinetics fitted better to a pseudo second order than pseudo first order thus confirming chemisorption. Adsorption data fitted better to Freundlich than Langmuir adsorption isotherm thus confirming monolayer adsorption. CPNCs successfully removed fluoride from aqueous solution though it could not remove fluoride to below WHO standards.

CHAPTER SIX

Recommendations for future work

The work in this project presents a basic understanding for clay polymer nanocomposites synthesis and the adsorption of Fluoride on CPNCs in batch adsorption. Future batch or column studies should incorporate the design and composition of more compatible polymers to clay as well as an understanding of the effects of various thermal and shear properties of polymers on fluoride removal should be studied.

Additional information is also needed to further understand realistic field condition as data presented was collected using fluoride solutions prepared from deionized water. Future equilibrium and batch studies should be conducted with a stock solution that mimics natural ion concentrations found in groundwater. This analysis will allow for more appropriate predictions to be made regarding the capacity and kinetics of the CPNCs in their proposed application. Future work should also incorporate realistic scaled flow rates, periodic flow, and synthetic groundwater and testing of fluoride adsorption on CPNC using columns under similar conditions to those observed in groundwater.

References

Anirudhan, T.S., and Ramachandran, M., (2008), Synthesis and characterization of amidoximated polyacrylonitrile/organobentonite nanocomposite for Cu((□), Zn(□), and Cd(□) adsorption from subtitkaqueous solutions and industry wastewaters. Ind. Eng. Chem> Res 47,6175-6184, pp.3

AWWA, (1999) *Water Quality and Treatment*: A Handbook of Community Water Supplies. McGraw-Hill, New York

Bhatnagar, A., Kumar, E., and Sillanpaa, M. (2011) *Fluoride removal from water by adsorption* – A review. Chemical Engineering Journal, 171 811-840

Brown, Jr. R. M., Saxena, I. M., and Kudlicka, K., (1996) *Cellulose biosynthesis in higher plants.* Trends in Plant Science, Elsevier Trends J, 2. pp. 149 - 156

Bochek, A. M., (2003) *Effect off hydrogen bonding on cellulose solubility in aqueous and non-aqueous solvents*, Russ. J. Appl, Chem. 76 pp. 1711 - 1719

Boruff, C.S., (1943) *Removal of Fluoride from Drinking Waters*. Ind. Eng. Chem. 26(1): pp. 69-71

Chen, W., Xu, R., Guanghua, C., Jzao, J., and Tichong, C., (1993) Changes of the prevalence of endemic fluorosis after changing water sources in two villages in Guangdong, China. Bull. Environ. Contam Toxicol, 479-482., pp. 51

Chen, H., (2014) *Chemical Composition and Structure of Natural Lignocellulose, Biotechnology of Lignocellulose: Theory and Practice*. Chemical Industry Press, Beijing and Springer Science + Business Media Dordrecht, DOI 10.1007/978-94-007. pp. 25 - 30

Chen, L., Bo-Yang, H., Shuai, H., Ting-Jie, W., Chao-Li, S., and Yong, J., (2011) *Fe-Ti oxide nano-adsorbent synthesized by co-precipitaion for fluoride removal from drinking water and its adsorption mechanism*, Powder Technology, Department of Chemical Engineering, Tsinghua University, Beijing 100084, China. pp. 1

Clair, N.S., Perry, L.M., and Gene, F.P., (1994) Chemistry for Environmental Engineering, Fourth Edition, McGraw -Hill. International editions. pp. 583-585

Delhom, C.D., White-Ghoorahoo, L.A., and Pang, S.S., (2009), Development and characterization of cellulose/clay nanocomposites, United States Department of Agriculture, Agricultural Research Service, Composites: Part B 41 (2010) 475–481, USA. pp. 2

Emerton, H.W., (1980). *The preparation of pulp fibers for papermaking*. In Handbook of Paper Science, Vol 1, The Raw Materials and Processing of Papermaking, Rance, H.F. (Ed.), Elsevier Scientific Publishing Company, The Netherlands, pp. 139-164.

Fayazi, M., (1994) Regional groundwater investigation on the Northern Springbok flats. Department of Water Affairs and Forestry. Geohydrology, GH Report no. 3684 108-155. pp. 18

Gaciri, S.J., and Davies, T.C., (1993), The occurrence and geochemistry of fluoride in some natural waters of Kenya. Journal of hydrology. 143(3-4) 395-412, pp. 14

Ghebreselassie, H., (2013) *Measuring the hydrophobicity of cellulose and the effect of humidity by inverse gas chromatography*. Indiana University of Pennsylvania, School of Graduate Studies and Research Department of Chemistry

Gupta, V.K., Ali, I., and Kumar Saini, V., (2007) *Defluoridation of wastewaters using waste carbon slurry*, Water Research, Volume 41, Issue 12. pp. 4

Hartman, H., Sposito, G., Yang, A., Manne, S., Gould, S.A.C., and Hansma, P.K., (1990) *Molecular-scale imaging of clay mineral surfaces with the atomic force microscope*, Clays and Clay Minerals, Vol. 38, No, 4. pp. 2

Hichour, Mustapha, Françoise P., Sandeaux, J., (2000) *Fluoride removal from waters by Donnan dialysis*, Separation and Purification Technology 18, 1: 1-11

Kickelbick, G., (2007), Hybrid Materials: *Synthesis, Characterization And Applications*. Wiley-VCH, pp. 7

Lepoittevin, B., Devalckenaere, M., Pantoustier, N., Alexandre, M., Kubies, D., Calberg, C., Jerome, R., and Dubois, P., (2002) Poly(Ɛ-caprolactone)/clay nanocomposites prepared by melt intercalation: mechanical, thermal and rheological properties. Laboratory of Polymeric and Composite Materials (SMPC), University of Mons-Hainaut, Place du Parce 20, Vol. 43. pp. 2

Maloney, T.C., (2000), *On the pore structure and dewatering properties of the pulp fiber cell wall.* Doctoral Thesis, Helsinki University of Technology, Finland.

Mandinic, Z., Curcic, M., Antonijevic, B., Carevic, M., Mandic, J., Djukic-Cosic, D, D., and Lekic, C.P., (2010), *Fluoride in drinking water and dental fluorosis*. *Sci, Total Environ*. 408. pp.

M'Caffrey, L.P., and Willis, J.P., (1993) Distribution of fluoride-rich groundwaters in the eastern parts of Bophuthatswana, relationship to bedrock and soils and constraints on drinking water supplies: a preliminary report, Africa Needs Ground Water. An International Ground Water convention. 11-8.

Mroczek, E.K., (2005) *Geothermics*, 43, pp. 218

Ncube, E. J., (2002) *The Distribution of Fluoride in South African Groundwater and the Impact thereof on Dental Health*. M.Sc. dissertation submitted to the University of Pretoria.

Oke, K., Neumann, S., and Adams, B., (2011) *Selective Fluoride Removal*, Water Today, India. pp. 2 - 3

Olad, A. (2011), *Polymer/Clay Nanocomposites*, Nanotechnology and Nanomaterials. University of Tabriz, Iran. DOI: 5772/14464. pp. 118 - 124

Oliveira, M. and Machado, A.V., (2013), *Preparation of Polymer-Based Nanocomposites by Different Routes*, Institute for Polymers and Composites, Department of Polymer Engineering, University of Minho, 4800-058, pp. 3 – 5

Pandey, N., Shukla, S.K., and Singh, N.B., (2017), Water purification by polymer nanocomposites: an overview, Nanocomposites, 3:2, 47-66, DOI: 10.1080/20550324.2017.1329983., pp. 18

Rong, M.Z., Zhang, M.Q., Zheng, Y.X., Zeng, H.M. and Friedrich, K., (2001), *Improvement of Tensil Properties of Nano-SiO_2/PP composite in relation to percolation mechanism*. Polymer42, 3301-3304. pp. 134

Ruiz-Hitzky, E., Aranda, P., Darder, M., and Ogawa, M., (2011), *Hybrid and biohybrid silicate based materials: molecular VS block-assembling bottom-up processes*. Chem.Soc. Rev 40,. pp. 6

Saha, H., (1993), Treatment of aqueous effluent for fluoride removal. Water Resolution, 27 (8) 134-1350., pp. 8

Scallan, A.M. and Carles, J.E., (1972), *The correlation of water retention value with fiber saturation point*. Svensk Papperstidn. **75** 699-703.

Sanchez, C., Julian, B., Belleville, P. and Popall, M., (2005), *Application of hybrid organic-inorganic nanocomposite*. J. Mater. Chem. 15, 3559-3592, pp. 12

Schadler, L.S., (2004), Polymer-Based and Polymer-filled Nanocomposites. *Nanocomposite science and Technology:*Wiley-VCH. 77-153, pp. 5 – 21

Shah, R.D., Kabadi, L.M., Pope, D.G., Augsburger, L.L., (1994), *Physicomechanical characterization of the extrusion-spheronization process*. I. Instrumentation of the extruder. Pharm. Res. 11, 355–360.

Singla, P., Mehta, R., and Upadhyay, S.N., (2012) Clay Modification by the Use of Organic Cations. Green and sustainable Chemistry, Department of Chemical Engineering, Thapar University, Patiala, India. 2. pp. 21 – 25

Sölener, M., Tunalib, S., Özcanc, A., Gedikbey, T., (2008), Adsorption characteristics of lead(□) ions onto the clay/poly(methoxyethyl)acrylamide (PMEA) composite from aqueous solutions. Desalination 223. pp. 8

Sonanglio, D., Bataille, B., Ortigosa, C., Jacob, M., (1995), *Factorial design in the feasibility of producing Microcel MC 101 pellets by extrusion/spheronization*. Int. J. Pharm. 115, 53–60.

Srimurali, M., (1998) *A study on removal of fluoride from drinking water by adsorption onto low cost materials*, Environmental Pollution, 99(2), 285-271.

Srinivasan, R., (2011), Advances in Application of Natural Clay and Its Composites in Removal of Biological, Organic, and Inorganic Contaminants from Drinking Water, Advances in Materials Science and Engineering, Hindawi Publishing Corporation, Article ID 872531. pp. 1 - 2

Strawhecker, K.E., and Manias, E., (2000), *Macromolecules*, Chem. Mater, 2943, pp. 12

Suprakas, S.R., and Masami, O., (2003), *Polymer/layered nanocomposites: a review from preparation to processing*, Advanced Polymeric Materials Engineering, Graduate School of Engineering, Japan. 468 8511.

Unuabonah, E.I., and Taubert, A., (2014), Clay-polymer nanocomposites (CPNCs): Adsorbents of the future for water treatment, Applied Clay Science, Institute of chemistry, university of Potsdam, Karl-Liebknecht-Str.24-25, D-14476 Potsdam, Germany, pp. 1

Vaia, R.A., and Giannelis, E.P., (1997) *Macromolecules*, 30

Valdez-Jimenez, L., SoriaFregozo, C., Miranda Beltran, M.L., Gutierrez Coronado, O., and Perez Vega, M.I., (2011), *Effects of the fluoride on the central nervous system*. Neurologia, 26. pp.

Vimonses, V., Jin, B., Chow, C.W.K., and Saint, (2009), Cost-effective adsorbents for removal of Congo-red in wastewater., Appl. Clay Sci. pp. 43

Viswanathan, G., Gopalakrishman, S., and Siva Ilango, S., (2010), *Assesssment on water contribution on total fluoride intake of various age groups of people in fluoride endemic and non-endemic areas of Dindigul District, Tamil Nadu, South India*. Water Res 44, 6186-6200. pp. 24

Weise, U., (1997), *Characterization and mechanism of changes in wood pulp fibers caused by water removal.* Doctoral Thesis, Helsinki University of Technology, Finland.

Whiteford, G.M., (1997), The metabolism and toxicity of fluoride, Karger, Basel. pp. 156

WHO (l984a) Guidelines for drinking water quality, Recommendations, 2nd edition Geneva 1

WHO (l984b) Fluorine and fluorides: Environmental Health criteria. World Health Organization Publication, Geneva, Switzerland. 36:364p.

World Health Organisation, (2002), *Fluorides* – Environmental Health Criteria 22: Geneva, Switzerland. pp.

WRC (2001) Distribution of fluoride-rich groundwater in the Eastern and Mogwase regions of the Northern and North-West provinces. WRC Report No. 526/1/01 South Africa: 1.1-9.85. pp 4

Zeronian, S.H., (1985), *Intercrystalline swelling of cellulose*, Cellulose Chemistry and Its Applications, Nevell T.P. and Zeronian S.H. (Eds), Ellis Horwood Limited, Great Britain, pp.138-158.

Zhang, J., Manias, E., and Wilkie, C.A., (2008) *Polymerically Modified Layered Silicates: An Effective Route to Nanocomposites*, Journal of Nanoscience and Nanotechnology, Vol. 8, 1597 – 1615, pp. 1.